

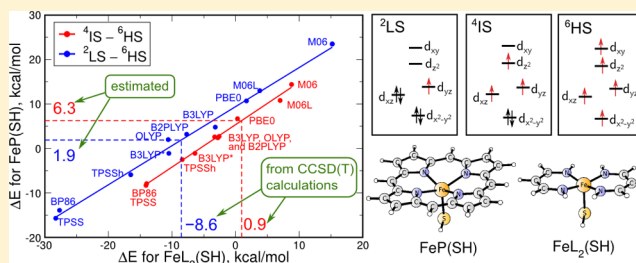
Spin-State Energetics of Heme-Related Models from DFT and Coupled Cluster Calculations

Mariusz Radoń*

Faculty of Chemistry, Jagiellonian University in Kraków, ul. Ingardena 3, 30-060 Kraków, Poland

S Supporting Information

ABSTRACT: Spin-state energetics of metalloporphyrins and heme groups is elucidated by performing high-level coupled cluster calculations for their simplified mimics. An efficient computational protocol is proposed—based on the mix of extrapolation to complete basis set and explicitly correlated (F12) methodology—which retains the high accuracy of the CCSD(T) method at a cost that makes it applicable also to relatively large models, e.g., FeP and FeP(Cl) (P = porphyrin). Adequacy of CCSD(T) is supported by analysis of multi-reference character and comparison with the completely renormalized CR-CC(2,3) method. The high-level coupled cluster results are used for assessment of density functional theory (DFT) methods, for which an accurate description of the spin-state energetics is recognized as a major challenge. Although the DFT results are highly functional-dependent, it is shown that the spin-state energetics of a full heme model and its simplified mimic remain in a good linear correlation. This makes it possible to estimate the spin-state energetics of full heme models based on the accurate CCSD(T) results for their mimics, as illustrated for porphyrin complexes of Fe(II), Mn(II), and Co(II); pentacoordinate heme complexes of Fe(II) and Fe(III); and a ferryl heme model. Comparison with the available experimental data is also presented.



1. INTRODUCTION

Spin states of transition metal complexes and enzymatic active sites—as determinants of their magnetic properties and many reactivity aspects—are in the focus of (bio)inorganic chemistry, catalysis, and materials science.^{1–4} However, it is a grand challenge for quantum chemistry methods to accurately compute the *spin-state energetics* (i.e., relative energies of the alternative spin states).⁴ This ability is needed not only to identify the ground spin state and a possibility of spin crossover, but also because the spin-state energetics strongly affect reactivity patterns observed in enzymatic and catalytic processes.^{1,4} Thus, for processes leading to a change of the spin state (e.g., some exchange-enhanced reactivities of metal-oxo species,¹ ligand binding to heme^{3b,5,6a}), the spin-state conversion energy contributes significantly to the thermochemical and kinetic parameters. In contrast, if an energy gap separating the alternative spin states is substantial, the reaction proceeds exclusively on the ground state energy surface.⁷

Although density functional theory (DFT) is currently a method of choice in most computational studies,^{8–10} the quality of the DFT spin-state energetics is not always satisfactory: the relative energies can vary a lot (~10–20 kcal/mol) when switching from one approximation of exchange-correlation functional to another.^{11,12} Although various functionals have been recommended by different research groups, it is difficult to achieve a high and systematic accuracy in the DFT calculations of transition metal spin-state energetics.^{4,13} Such a situation stimulates a noticeable interest

in performing correlated ab initio calculations that could provide reliable spin-state energetics to be used for assessment of the DFT accuracy, picking the best functionals, and clarifying more problematic cases (see refs 12–15 for review and refs 16–23 for selected applications). One should note, however, that correlated ab initio calculations for transition metal complexes are expensive (thus often applicable only to simplified models) and methodologically challenging.

Transition metal complexes are strongly correlated systems, for which a nondynamical correlation can play a major role even in the equilibrium geometry.²⁴ This correlation can be covered most elegantly by *multireference methods*, for instance, a complete or restricted active space approach (CASSCF/CASPT2, RASSCF/RASPT2);²⁵ for the scope of applications, see ref 26. But unless the multireference character is extremely pronounced, the alternative and robust approach is to use *single-reference coupled cluster methods*. Even though they are based on a poor reference wave function (single Slater determinant), all the correlation effects can be described appropriately, provided that excitations of sufficiently high order are included in an expansion of the cluster operator.²⁷ In view of the previous studies,^{15,23} at least an approximate (noniterative) treatment of connected triples is necessary for a balanced description of transition metal spin-state energetics. This leads to the choice of the CCSD(T) method, which is

Received: February 7, 2014

Published: May 2, 2014

often regarded a “golden standard” of accuracy for a variety of chemical problems,²⁷ including also transition metal thermochemistry.^{15,23,28–30}

However, apart from possible deficiencies due to multi-reference character, a major obstacle in performing reliable coupled cluster calculations is the computational cost that rapidly increases with the system size, the basis set, and the level of excitations included in the cluster operator.¹⁵ Although the most recent, locally correlated, implementations of the coupled cluster theory^{31,32} look very promising and may circumvent many of these limitations in the near future, it is still far from trivial to perform accurate coupled cluster calculations for open-shell transition metal complexes.

A good example is metalloporphyrins and heme groups, to which this study is devoted. These heme-related models are interesting not only for their biological significance but also for an unusual spin-state versatility: the ground state can be either a low-spin (LS), a high-spin (HS), or an intermediate-spin (IS) state, depending on the metal and character of the axial ligand(s), and is known to change in the course of biologically relevant processes, such as ligand binding.^{3b,5,6a,13} However, a large size of the porphyrin ring makes these systems challenging for computational treatment at the coupled cluster level.

In order to approach accurate spin-state energetics of metalloporphyrins and heme groups, high-level CCSD(T) calculations will be reported here for their simplified mimics, with the aim of providing benchmark-quality results. The mimics are constructed by replacing the porphyrin by appropriate N-donor ligands (described in section 2), leading to similar models as used in the previous studies by Harvey et al.,¹⁹ Ghosh et al.,¹⁶ Johansson and Sudholm,³³ and Scherlis and Estrin.³⁴ Among two possible choices of the mimicking ligand (CN_2H_3^- or $\text{C}_3\text{N}_2\text{H}_5^-$) the present work is mainly focused on the second and larger one—devised to better simulate a ligation of the metal by the porphyrin ring. Moreover, much larger basis sets will be used here than in the previous coupled cluster calculations,^{16,19} and the effects of the metal outer-core (3s,3p) correlation will be consistently included. Attention will be also paid to multireference character and its prospective consequences for the energetics.

After examining a basis set dependence of the relative CCSD(T) spin-state energetics, a reliable and efficient computational protocol will be proposed. The new protocol, thanks to an economic use of the basis set and due to benefits from the explicitly correlated approach (F12),³⁵ can be applied not only to a variety of small mimics, but also (directly) to selected porphyrin complexes. It will be also shown that the high-level calculations for the simplified mimics can be used to estimate the spin-state energetics of the corresponding heme models, even if accurate calculations for the latter species may be presently too demanding. Employing this approach, the spin-state energetics of selected metalloporphyrins, pentacoordinate heme complexes, and a ferryl heme model will be discussed vis-à-vis the coupled cluster results for their small mimics and the available experimental data. Performance of selected DFT methods will be evaluated with respect to the CCSD(T) results and estimates.

2. MODELS AND THEIR SPIN STATES

The following complexes were studied by means of DFT calculations (where P stands for porphyrin, Im for imidazole): $\text{Fe}^{\text{II}}\text{P}$, $\text{Mn}^{\text{II}}\text{P}$, $\text{Co}^{\text{II}}\text{P}$, $\text{Fe}^{\text{II}}\text{P}(\text{Im})$, $[\text{Fe}^{\text{II}}\text{P}(\text{CN})]^-$, $\text{Fe}^{\text{III}}\text{P}(\text{Cl})$, $\text{Fe}^{\text{III}}\text{P}(\text{SH})$, and $\text{FeO}(\text{P})(\text{Cl})$ (with a ferryl group); herein

these models with a porphyrin ligand will be called *full heme models*. The corresponding coupled cluster calculations were performed mostly for their simplified *mimics*—in which the porphyrin ring was replaced by two bidentate, N-donor ligands: either small amidines CN_2H_3^- (abbrev. A) or somewhat larger ligands $\text{C}_3\text{N}_2\text{H}_5^-$ (abbrev. L). The structures of the full heme model and its mimics of the two types (A_2^- and L_2^- -based) are shown in Figure 1 on the example of iron(II) porphyrin; for

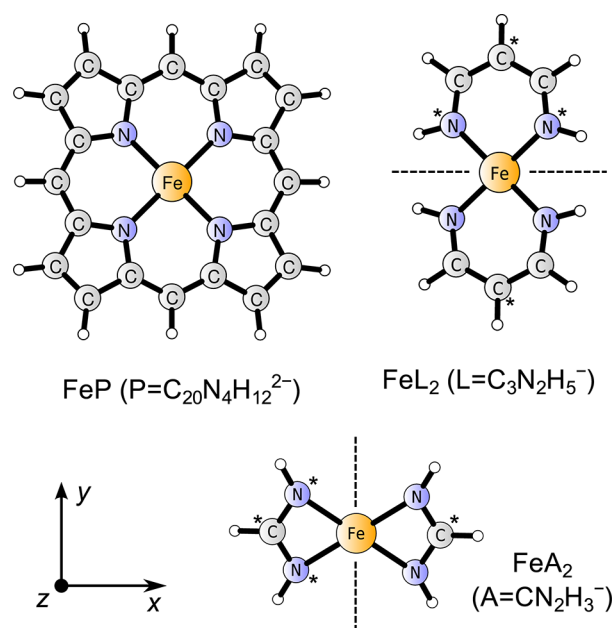


Figure 1. Full heme model (FeP), its two small mimics (FeL_2 , FeA_2), and their orientation in the Cartesian coordinate system on the example of an iron(II) porphyrin complex. Dashed lines show the positions of mirror planes in analogous mimics with C_s symmetry [e.g., $\text{FeL}_2(\text{SH})$]. Atoms marked by asterisks define the dihedral angle ($\text{N}-\text{C}-\text{N}-\text{C}$) whose value was frozen in order to keep the planarity of the two A or L ligands (see text).

other heme complexes the mimics were constructed analogously (note that the axial Im was replaced by NH_3 ; for the ferryl model only the L_2 -based mimic was considered). Similar mimics have been used in the previous studies, where this approach was introduced and validated.^{16,19,21,33,34}

A consistent orientation of the models in the coordinate system is assumed, as shown in Figure 1. In this orientation, the $d_{x^2-y^2}$ orbital is essentially nonbonding, in contrast to d_{xy} , which is the one most strongly destabilized by interaction with the ring (equatorial) ligand. More precisely, the metal d_{xy} orbital participates in the σ -type metal–ligand bonding by overlap with the appropriate combination of the lone pairs on the four coordinating nitrogen atoms;^{26b} the orbital formally labeled as d_{xy} is, in fact, the antibonding orbital (σ_{xy}^*). The d_z orbital has either antibonding character (σ_z^*) or nonbonding character, depending on whether the axial ligand is present or not. The d_{xz} and d_{yz} orbitals, whose contours are perpendicular to the ring, are essentially nonbonding with respect to the ring but may be involved in π -bonding interactions with the axial ligand: slightly in the case of Cl^- and SH^- , more substantially in the case of an oxo group. Note that for the structures with a 4-fold symmetry axis, the d_{xz} and d_{yz} orbitals are degenerate; for the remaining structures (assuming the orientation as in Figure 1), the d_{xz} orbital has lower energy than the d_{yz} one. Note also that in the

case of FeP(Im) the optimum orientation of the Im ring (coincident with the symmetry plane) is different for the quintet state (i.e., the $y = 0$ plane) than for the triplet and singlet spin states (i.e., the $x = y$ plane), cf. ref 20. Thus, for the quintet state the natural orbitals are not d_{xz} , d_{yz} but their combinations $d_{||}$, d_{\perp} , whose contours are parallel or perpendicular, respectively, to the Im ring

The spin states of full heme models and the corresponding spin states of their small mimics are described in Table S1 (Supporting Information) by giving the electronic configurations (formal occupancies of the d orbitals) and the term symbols. However, as the term symbol is usually different for a full heme model than for its small mimic, the spin states will be consistently labeled as LS (low-spin), IS (intermediate-spin), or HS (high-spin) with the spin multiplicity indicated in the superscript. For instance, the ${}^6\text{HS}$ state is ${}^6\text{A}_{1g}$ for MnP but ${}^6\text{A}_g$ for ML_2 and MA_2 (cf Table S1). Two close-lying triplet states of FeP are labeled as ${}^3\text{IS}_1$ and ${}^3\text{IS}_2$ —the first being the orbitally nondegenerate (${}^3\text{A}_{2g}$) and the second the orbitally degenerate state (${}^3\text{E}_g$). The same convention is used for the doublet and quartet states of CoP and MnP, as well as for the corresponding spin states of their mimics. Note that (like in the previous study^{6a}) the ${}^1\text{LS}$ state considered below for FeP and its small mimics is the closed-shell singlet state (${}^1\text{A}_{1g}$) analogous to the singlet state of FeP(Im), and not the lower-energy open-shell singlet state arising from the same electronic configuration as the ${}^3\text{IS}_1$ state.³⁶

In order to provide adiabatic spin-state energetics, the structure was optimized separately for each spin state. For spatially degenerate states, Jahn–Teller distortion was taken into account by performing the optimization in an appropriate symmetry subgroup (D_{2h} for ${}^3\text{IS}_2$ of FeP, ${}^4\text{IS}_2$ and ${}^2\text{LS}_2$ of MnP, and ${}^2\text{LS}_2$ and ${}^4\text{HS}_2$ of CoP; C_{2v} for ${}^2\text{LS}$ of FeP(Cl) and ${}^3\text{IS}$ of $[\text{FeP}(\text{CN})]^-$; C_s for ${}^5\text{HS}$ of $[\text{FeP}(\text{CN})]^-$). Note also that, like in the previous studies,^{19,21} the necessary constraints were imposed on the structures of the small mimics in order to keep the planar arrangement of the four nitrogen atoms (to resemble the metal ligation by porphyrin). This was achieved either by assuming the D_{2h} symmetry for ML_2 , MA_2 ($M = \text{Fe}, \text{Mn}, \text{Co}$), or by freezing the appropriate dihedral angle (the one indicated in Figure 1) for the other (less symmetric) mimics.

3. COMPUTATIONAL DETAILS

3.1. DFT Calculations. The DFT calculations were carried out with Turbomole,³⁷ except for the exchange-correlation functionals not available in this program and for the relativistic calculations, for which Gaussian 09³⁸ was used. All open-shell DFT calculations were spin-unrestricted.

The structures were optimized with the def2-TZVP³⁹ basis set and the BP86 functional, except for FeP and its small mimics, whose structures used in the calculations below are those optimized with the B3LYP functional. This minor difference is not expected to alter the energetics significantly, as, for FeP, the relative DFT spin-state energetics is nearly insensitive to the choice of either the BP86 or the B3LYP structures (see Table S2, Supporting Information), consonant with observations by other authors that choosing a particular DFT method is far less important for the structure optimization than for the energetics.⁴⁰

As the DFT spin-state energetics were reported to be quite sensitive to the basis set,⁴¹ the final DFT energetics were calculated using a larger basis set: composed of def2-QZVPP⁴² on the metal and def2-TZVPP⁴³ on the ligand atoms. A

number of exchange-correlation functionals were used at this stage, including hybrid functionals (B3LYP,⁴⁴ PBE0,⁴⁵ B3LYP*,⁴⁶ TPSSH⁴⁷), the classical GGA (BP86⁴⁸) and meta-GGA (TPSS⁴⁹) functionals, the OLYP functional,⁵⁰ the double-hybrid functional (B2PLYP⁵¹), as well as two Minnesota functionals (M06, M06L).⁵² Some of these functionals have been previously recommended by various authors in the context of spin-state energetics.^{46,53–56} An estimate of scalar-relativistic effects at the second-order Douglas–Kroll (DK) level⁵⁷ was included in the DFT spin-state energetics (see Table S2, Supporting Information). These estimates were determined for the B3LYP* functional—by comparison of the DK-relativistic energetics (basis set: cc-pVQZ-DK/cc-pVTZ-DK for metal/ligand atoms) with the nonrelativistic one (basis set: cc-pVQZ/cc-pVTZ for metal/ligand atoms)—and used to correct the results from other DFT methods.

3.2. Coupled Cluster Calculations. Single point CCSD-(T) calculations were performed with Molpro⁵⁸ and (unless stated otherwise) refer to the partially spin adapted ROHF/RCCSD(T) approach, in which the linear part of the wave function is an eigenfunction of \hat{S}^2 .⁵⁹ A comparison with the alternative ROHF/UCCSD(T) approach will be provided below for a few representative cases. The completely renormalized coupled cluster calculations at the CR-CC(2,3) level (D version of the correction)⁶⁰ were performed with GAMESS (rev. May 2012).⁶¹ All the coupled cluster calculations reported in this work are either scalar-relativistic at the second-order DK level⁵⁷ and simultaneously correlating the metal outer-core (3s,3p) electrons (rcc, from “relativity and core correlation”) or nonrelativistic with the metal outer-core frozen (nrfc, from “non-relativistic frozen-core”). The cores of ligands and the inner-core of the metal (up to 2p) were frozen in all cases.

A number of basis sets were used. In addition to those of uniform nZ quality on all atoms, which are compactly denoted by n (i.e., T, Q, or S), also *composite basis sets* were considered, in which a larger basis set was used for the metal or the metal with its first coordination sphere than for the remaining atoms. These two types of composite basis sets are denoted as m/n or $m(n)$, respectively, where $m(n)$ is a basis set of mZ quality for the metal and of nZ quality of the remaining atoms and $m(n)$ is a basis set of mZ quality for the metal and atoms in the first coordination sphere and of nZ quality for the remaining atoms [m, n stand for the basis set cardinal numbers (D, T, Q, S); $m \geq n$]. Note that for models with an axial cyanide ligand, the same basis set is used for the N as for the C atom (as if both atoms belonged to the first coordination sphere).

Except for F12 calculations (see below), Dunning-type correlation-consistent basis sets⁶² were used: either cc-pwCVnZ-DK/cc-pVnZ-DK (for metal/ligand atoms, respectively) in the case of rcc calculations or the standard cc-pVnZ in the case of nrfc calculations. For instance, the composite basis set T(D) used in the rcc calculations is composed of cc-pwCVTZ-DK for the metal and cc-pVTZ-DK for the first coordination sphere and cc-pVDZ-DK for the remaining ligand atoms. This T(D) basis set should be distinguished from a smaller T/D one, in which cc-pVDZ-DK is used for all the ligand atoms. The analogous T(D) and T/D basis sets for the nrfc calculations are composed of cc-pVTZ and cc-pVDZ, respectively.

Extrapolation of correlation energy to the complete basis set (CBS) limit was performed according to the Helgaker two-point formula⁶³

$$E_{\text{corr}}^{[m_1:m_2]} = \frac{m_2^3 E_{\text{corr}}(m_2) - m_1^3 E_{\text{corr}}(m_1)}{m_2^3 - m_1^3} \quad (1)$$

based on the correlation energies recovered with correlation consistent basis sets of cardinal numbers m_1 and m_2 ; the SCF energy was taken from the larger basis set. The extrapolations using the basis sets of uniform quality for all atoms are denoted as $[m_1:m_2]$, such as [T:Q]. In the case of composite basis sets m/n and $m(n)$, the extrapolation according to eq 1 was only performed with respect to basis set denoted by m (i.e., on the metal or the metal and its first coordination sphere), while keeping the basis set denoted by n (i.e., on the remaining atoms) fixed. The resulting extrapolated energies are denoted as $[m_1:m_2]/n$ or $[m_1:m_2](n)$, such as [T:Q]/D and [T:Q](D), depending on the treatment of atoms in the first coordination sphere.

Explicitly correlated³⁵ CCSD-F12 calculations were performed (only at the nrfc level) within the CCSD-F12a and CCSD-F12b approximations by Werner et al.,⁶⁴ as implemented in Molpro. The default value of the geminal exponent was used, $\beta = 1.0$. The explicitly correlated wave function was constructed according to ansatz 3 of ref 65, with either fixed amplitudes determined from the cusp condition (FIX) or diagonal amplitudes determined by a preceding MP2-F12 step (D).⁶⁶ Thus, the methods used are denoted as CCSD-F12 $x(y)$, where $x = a$ or b denotes the approximation and $y = \text{FIX}$ or D denotes the amplitude ansatz. The general ansatz (G) was also tested, although in most cases numerical problems were encountered already at the MP2-F12 step, preventing us from continuing with this approach. However, in a few cases where the calculations were doable, the general ansatz gave results close to the diagonal ansatz (Tables S11 and S12, Supporting Information).

The CCSD-F12 calculations were performed with the T and T(D) basis sets (see above for the notation) constructed from the Karlsruhe def2-TZVPP (TZ quality) and def2-SVP (DZ quality) basis sets.^{39,43} The corresponding MP2FIT auxiliary basis sets⁴³ were used for density-fitting of Coulomb integrals while the JKFIT auxiliary basis sets⁶⁷ were used for density-fitting of exchange integrals and for resolution-of-identity (RI) approximation of many-electron integrals. For comparison, correlation consistent orbital basis sets (cc-pVTZ, aug-cc-pVTZ, in combination with suitable auxiliary basis sets⁶⁸) were tested in a few cases, providing similar results (see Tables S11 and S12, Supporting Information). Likewise, using larger auxiliary basis sets (in particular, for the RI) does not improve the results significantly (Tables S11 and S12) and appears (from our experience) less important than the choice of the ansatz or the approximation.

As will be mentioned in section 4.4.4, the CCSD-F12 calculations for FeO(L₂)Cl were carried out using the Kohn–Sham orbitals instead of the canonical HF orbitals. Therefore, to be consistent with the Molpro implementation, a single iteration of standard SCF calculations (not allowed to change the molecular orbitals) was executed prior to the CCSD-F12.⁶⁹

In all cases, the standard CABS singles correction was added to the reference energies. The effect of this correction on the relative spin-state energetics depends on the system and spin-state, varying from a negligible 0.1–0.2 kcal/mol to nearly 1 kcal/mol; the effect is comparable for HF and KS orbitals (cf Table S19, Supporting Information).

4. RESULTS AND DISCUSSION

4.1. Establishing the CCSD(T) Computational Protocol. As mentioned in the Introduction, an important objective of this work is to establish a computational protocol for calculation of transition metal spin-state energetics at the CCSD(T) level. The aim is to retain the high accuracy of the method in the complete basis set (CBS) limit, while keeping affordable the computational cost by an economic use of the basis set.

A large basis set is, in general, needed to recover the correlation energy appropriately. But because it makes the CCSD(T) calculations very expensive, a compromise is usually needed. As the change of spin state occurs mainly on the metal center, it is physically motivated to use a larger basis set for the metal, or for the metal with its first coordination sphere, than for the remaining atoms. This is the idea of composite basis sets denoted as m/n and $m(n)$, and the corresponding CBS extrapolation schemes, $[m_1:m_2]/n$ and $[m_1:m_2](n)$ introduced in section 3.2 (where the notation is explained). Similar basis sets and CBS extrapolations have also been used elsewhere,¹⁹ and this approach seems very attractive—especially the cheap extrapolation schemes, like [T:Q]/D, because the extrapolation is performed only with respect to a metal basis set, while fixing a small basis set on the other atoms. However, according to the author's knowledge, the accuracy of this approach has not been rigorously tested with respect to more reliable (large basis set) calculations in the context of spin state energetics. Results of such a benchmark are presented below. A similar benchmark will also be shown for the results of explicitly correlated (F12) calculations. Although the F12 calculations are very promising³⁵ and clearly useful for accurate transition metal thermochemistry,^{28,29} there are at the moment certain practical caveats when applying this approach to transition metal complexes—related to the treatment of relativistic effects, the (T) correlation energy, and the outer-core contribution to the correlation energy, as well as the optimal choice of orbital and auxiliary basis sets for transition metals.

Owing to the above issues and to efficiency reasons (see below), it is advantageous to split the relative CCSD(T) energetics into the following three contributions:

$$\Delta E_{\text{CCSD(T)}} = \Delta E_{\text{CCSD}}^{(\text{nrfc})} + \Delta \epsilon_{\text{CCSD}}^{(\text{rcc})} + \Delta E_{(\text{T})} \quad (2)$$

The first one is a nonrelativistic, frozen core (nrfc) approximation to the CCSD energetics, to which one can apply the CBS extrapolation as well as the F12 methodology. The second term corrects the first one for the effects of special relativity and core correlation (rcc), i.e.,

$$\Delta \epsilon_{\text{CCSD}}^{(\text{rcc})} = \Delta E_{\text{CCSD}} - \Delta E_{\text{CCSD}}^{(\text{nrfc})} \quad (3)$$

The third term is the standard noniterative correction for the connected triples contribution to the correlation energy (at the rcc level). For the lack of rigorous F12 implementations, the second and the third contributions can be obtained from CBS extrapolations.

Another motivation to discuss separately the three contributions in eq 2 is that they have (as will be shown) different convergence behavior with respect to the basis set. In order to determine optimal basis set requirements for each term, a comparison was made with a benchmark set of accurate relative energetics for the following eight small models: FeA₂, FeL₂, MnA₂, MnL₂, CoA₂, CoL₂, FeA₂(Cl), and FeA₂(NH₃). These models represent a variety of metals and axial ligands of

the heme-related models, but are still small enough to permit calculations with high quality basis sets. As such, the spin-state energetics for the benchmark set were obtained from the [Q:5](T) extrapolation. The results and detailed comparison with cheaper CBS extrapolation schemes and CCSD-F12 calculations are given in Supporting Information (Tables S3–S6); a summary and analysis is provided in Table 1. Further discussion of accuracy can be found in the Supporting Information.

Table 1. Accuracy of Various Methodologies in Reproducing Three Contributions to CCSD(T) Relative Spin-State Energetics^{a,b,c}

methodology ^d	MAE			Max		
	$\Delta S = 1$	$\Delta S = 2$	$\Delta S = 0$	$\Delta S = 1$	$\Delta S = 2$	$\Delta S = 0$
$\Delta E_{\text{CCSD}}^{\text{(nrfc)}}$ contribution						
[T:Q]/D	2.09	2.92	0.94	3.48	5.95	4.12
[T:Q](D)	0.35	0.58	0.33	0.83	1.06	0.59
[T:Q](T)	0.51	1.01	0.09	0.88	1.28	0.23
[T:Q] ^e	0.51	1.02	0.07	0.88	1.35	0.22
[Q:5]/D	4.04	5.98	1.40	9.17	10.46	5.12
[Q:5](D) ^e	0.19	0.26	0.25	0.89	0.87	0.66
F12a(FIX)/T	0.45	1.05	0.30	1.10	1.35	0.72
F12b(FIX)/T	1.05	2.40	0.19	2.02	3.00	0.42
F12a(D)/T	0.38	0.58	0.32	1.13	1.28	0.68
F12b(D)/T	0.21	0.31	0.25	0.66	0.57	0.49
F12b(D)/T(D)	0.36	0.52	0.37	1.58	1.36	0.83
$\Delta E_{\text{CCSD}}^{\text{(fcc)}}$ contribution						
[T:Q]/D	0.30	0.54	0.04	0.53	0.71	0.09
[T:Q](D)	0.12	0.24	0.02	0.19	0.31	0.07
[T:Q](T)	0.14	0.21	0.04	0.60	0.30	0.20
[Q:5]/D	0.04	0.05	0.02	0.11	0.16	0.10
$\Delta E_{\text{(T)}}$ contribution						
[T:Q]/D	0.21	0.26	0.20	0.68	0.63	0.47
[T:Q](D)	0.08	0.11	0.10	0.31	0.31	0.33
[T:Q](T)	0.03	0.06	0.01	0.25	0.32	0.03
[Q:5]/D	0.34	0.49	0.24	1.13	1.09	0.65

^aMean absolute error (MAE) and maximum error (Max) for relative energies of the spin states with $\Delta S = 1, 2$ and 0 from the benchmark set. ^bThe errors are given with respect to the [Q:5](T) energetics, all values in kcal/mol. ^cThe benchmark set includes: FeA₂, FeL₂, MnA₂, MnL₂, CoA₂, CoL₂, FeA₂(Cl), and FeA₂(NH₃). ^dCBS extrapolation scheme or CCSD-F12x(y) setup with a specified basis set, either T or T(D), where $x = a, b$ is the approximation, and $y = \text{FIX}, \text{D}$ is the ansatz (see section 3.2 for the notation of basis sets used and other methodology details). ^eCalculations at this level were not performed for FeA₂(NH₃).

As already mentioned, Table 1 summarizes the accuracy of various CBS extrapolation schemes (with respect to the [Q:5](T) extrapolation) in reproducing the three contributions to the relative spin-state energetics: $\Delta E_{\text{CCSD}}^{\text{(nrfc)}}$, $\Delta E_{\text{CCSD}}^{\text{(fcc)}}$, and $\Delta E_{\text{(T)}}$ in eq 2. For the first contribution, the accuracy of a few CCSD-F12 setups is additionally provided. The data in Table 1 are grouped according to a difference of the spin quantum number (ΔS) of the electronic states whose energies are compared. There are 32 pairs of spin states with $\Delta S = 1$ [e.g., ¹LS–³IS for Fe(II), ³IS–⁵HS for Fe(II)], eight pairs with $\Delta S = 2$ [e.g., ¹LS–⁵HS for Fe(II)], and 10 pairs with $\Delta S = 0$ [e.g., ³IS₁–³IS₂ for FeA₂ and FeL₂ models] in the present benchmark set. For each of these ΔS values in Table 1, the error statistics are reported separately.

Already the first glimpse at Table 1 reveals that the $\Delta E_{\text{CCSD}}^{\text{(nrfc)}}$ contribution is much more demanding in terms of basis set than other contributions in eq 2. Even for the full [T:Q] CBS extrapolation—the level which is already very expensive for the larger of our models—the CCSD relative energetics is still subject to ~ 1 kcal/mol basis set error. Clearly, it is much worse with the relative CCSD energies before extrapolation (Supporting Information), which are subject to basis set errors as large as 3–5 and ~ 2 kcal/mol for TZ- and QZ-quality basis sets, respectively. We notice that these large basis set errors are almost exclusively rooted in the CCSD correlation energies; basis set errors on the relative HF energies are much smaller, up to 0.6 kcal/mol for the TZ basis set and up to 0.2 kcal/mol for the QZ one.

The errors in CCSD energetics are particularly large (up to 3–6 kcal/mol) for the extrapolation scheme [T:Q]/D and even more serious (up to 10 kcal/mol) for the [Q:5]/D one. This illustrates how bad coupled cluster energetics can be if obtained from unbalanced basis sets. The problem with these composite extrapolations is evidently due to incompatibility of the large basis set on the metal atom (QZ, 5Z) with the much smaller one on the ligands (DZ). This seems to be mitigated by using the basis set of the same quality as for the metal also for the atoms in the first coordination sphere. Indeed, the [T:Q](D) extrapolation and especially the [Q:5](D) one clearly lead to a much better accuracy—obviously, at the expense of using the QZ- or 5Z-quality basis set for all atoms in the first coordination sphere. Note that, surprisingly, the CCSD relative energies from the [T:Q](D) extrapolation are in some cases more accurate than those from the [T:Q](T) or the full [T:Q] extrapolation; this behavior, if not rooted in minor inaccuracies in the reference data, is presumably due to some error cancellation which is not expected to be systematic.

Compared with the CBS extrapolations, the explicitly correlated CCSD-F12 calculations in Table 1 look very attractive concerning the balance between the accuracy and the efficiency.⁷⁰ Indeed, already with the TZ-quality basis set, the CCSD-F12 relative energetics can be more reliable than the energetics from the expensive [T:Q] extrapolation. Whereas the accuracy of CCSD-F12 is not bad for the default, fixed amplitude ansatz (FIX), it considerably improves for the diagonal ansatz (D). Thus, the CCSD-F12b(D) method becomes the preferred approach in this work. Interestingly, the accuracy does not degrade significantly if the T basis set is replaced with the T(D) one. Although this may seem obvious for the A₂-based models (where the difference between both basis sets is slight on two carbons and the hydrogen atoms), the same also holds true for the FeL₂ model. However, somewhat larger discrepancies (up to 1.6 kcal/mol) are observed for MnL₂ and CoL₂, affecting the maximum error statistics in Table 1. Since there are only three L₂-based models in the benchmark set, additional tests were carried out for FeL₂(NH₃) and FeL₂(Cl) (Supporting Information, Table S13); for these systems the discrepancies in the relative energetics between the T and T(D) basis sets are as small as 0.3 kcal/mol. Thus, we are strongly encouraged to use the composite basis set T(D) in the CCSD-F12 calculations, particularly for the iron models. But even the maximum errors for MnL₂ and CoL₂ are not serious in light of a low cost of the calculations and a possibility of applying this approach also to larger systems (see below), for which the full TZ basis set on the ligands may be too expensive.

As already mentioned above, the basis set errors are much smaller for two other contributions in eq 2: the $\Delta E_{\text{(T)}}$ and

Table 2. Relative CCSD(T) Spin-State Energetics of Small Mimics and Two Iron-Porphyrin Complexes (kcal/mol)^a

model	spin state	$\Delta E_{\text{CCSD(T)}}$		model	spin state	$\Delta E_{\text{CCSD(T)}}$	
FeA ₂	¹ LS	50.9	(50.6)	FeL ₂	¹ LS	29.8	(30.3)
	³ IS ₁	11.1	(11.4)		³ IS ₁	−6.2	(−6.3)
	³ IS ₂	15.5	(15.4)		³ IS ₂	−8.7	(−8.8)
	⁵ HS	0			⁵ HS	0	
MnA ₂	² LS ₁	76.3	(76.6)	MnL ₂	² LS ₁	28.0	(26.4)
	² LS ₂	56.2	(55.4)		² LS ₂	34.0	(32.4)
	⁴ IS ₁	27.5	(27.1)		⁴ IS ₁	10.8	(9.8)
	⁴ IS ₂	34.5	(34.4)		⁴ IS ₂	6.3	(5.3)
CoA ₂	⁶ HS	0		CoL ₂	⁶ HS	0	
	² LS ₁	0			² LS ₁	0	
	² LS ₂	−4.5	(−5.0)		² LS ₂	−6.9	(−7.7)
	⁴ HS ₁	−7.3	(−7.1)		⁴ HS ₁	12.7	(12.6)
FeA ₂ (NH ₃)	⁴ HS ₂	−5.8	(−5.4)	FeL ₂ (NH ₃)	⁴ HS ₂	12.5	(13.1)
	¹ LS	29.7	(29.5)		¹ LS	8.5	
	³ IS	16.6	(16.7)		³ IS	−3.6	
	⁵ HS	0			⁵ HS	0	
[FeA ₂ (CN)] [−]	¹ LS	29.4		[FeL ₂ (CN)] [−]	¹ LS	−0.9	
	³ IS	22.4			³ IS	2.7	
	⁵ HS	0			⁵ HS	0	
	² LS	30.3	(29.8)	FeL ₂ (Cl)	² LS	6.1	
FeA ₂ (Cl)	⁴ IS	10.5	(10.6)		⁴ IS	2.2	
	⁶ HS	0			⁶ HS	0	
	² LS	21.7		FeL ₂ (SH)	² LS	−8.6	
FeA ₂ (SH)	⁴ IS	10.6			⁴ IS	0.9	
	⁶ HS	0			⁶ HS	0	
	¹ LS	29.9		FeP(Cl)	² LS	14.7	
FeP	³ IS ₁	−2.3			⁴ IS	5.6	
	³ IS ₂	−0.6			⁶ HS	0	
	⁵ HS	0					

^aObtained from eq 2 using the adopted computational protocol. For reference, the results from the [Q:5](T) extrapolation are given in parentheses, wherever available. The spin states are labeled as LS (low-spin), IS (intermediate-spin), or HS (high-spin), with the spin multiplicity annotated in the superscript (cf. section 2).

$\Delta E_{\text{CCSD}}^{(\text{rcc})}$ terms. In fact, the first one is reasonably accounted for already by the cheapest of the tested extrapolation schemes, [T:Q]/D, in spite of its failure for the CCSD correlation energy (see above). Its good performance for the triples contribution (T) may simply follow from the fact that the (T) correlation energy is an order of magnitude smaller than the CCSD one. Obviously, the extrapolation schemes like [T:Q](D), [T:Q](T), or [T:Q] can reproduce the triples contribution to the correlation energy even more accurately (Table 1). But given that the (T) correction is usually the most expensive part of the CCSD(T) calculations (i.e., has the worst scaling and requires the most significant memory resources), the quality of the [T:Q]/D extrapolation should be considered satisfactory for the present purposes. A similar observation can be made for the $\Delta E_{\text{CCSD}}^{(\text{rcc})}$ contribution, which is not particularly sensitive to the basis set for the ligands, somewhat more to the one for the metal atom. This was to be expected as the $\Delta E_{\text{CCSD}}^{(\text{rcc})}$ contribution is predominantly of atomic origin. Consequently, the [Q:5]/D extrapolation, however inaccurate it was for the CCSD energetics, reproduces the correction $\Delta E_{\text{CCSD}}^{(\text{rcc})}$ nearly exact.

In sum, the performed comparison with the benchmark-quality CBS extrapolation [Q:5](T) has suggested the following protocol for computation of the relative spin-state

energetics at the CCSD(T) level, as a trade-off between accuracy and efficiency:

- The $\Delta E_{\text{CCSD}}^{(\text{nrfc})}$ contribution is obtained from the nrfc CCSD-F12b(D)/T(D) calculations.
- The correction term $\Delta E_{\text{CCSD}}^{(\text{rcc})}$ is obtained from the [Q:5]/D extrapolations (by subtracting the CCSD energetics at the rcc and nrfc level).
- The $\Delta E_{\text{(T)}}$ term is obtained from the [T:Q]/D extrapolation (at the rcc level).

The main advantage of this approach is that the vastness of basis set error is minimized by the F12 methodology, while use of a large basis set is avoided for the expensive (T) contribution. Consequently, this protocol can be applied not only to simplified mimics but also to larger complexes, as will be illustrated below for FeP and FeP(Cl). Clearly, calculations for the latter species are significantly more expensive than for the mimics (e.g., the total CPU time needed to compute a single spin state of FeP(Cl) was about 60 days, see Table S14, Supporting Information). It is helpful that calculations in the present computational protocol can be split into independent tasks, which can run in parallel if only sufficient resources are available.

4.2. CCSD(T) Energetics. Relative CCSD(T) spin-state energetics resulting from the adopted computational protocol are reported in Table 2 (except for the FeO(L₂)Cl model,

which is covered in section 4.4.4). The reference results from the [Q:5](T) extrapolation are also given for comparison, wherever available; as was concluded in section 4.1, both CCSD(T) energetics fall in a good agreement (maximum discrepancy 1.6 kcal/mol, for most cases less than 1 kcal/mol).

While only the final CCSD(T) energetics are given in Table 2, the three contributions determined in the computational protocol ($\Delta E_{\text{CCSD}}^{\text{nrfc}}$, $\Delta E_{\text{CCSD}}^{\text{rcc}}$, $\Delta E_{\text{(T)}}$) can be found in Table S16, Supporting Information. It follows that the rcc correction ($\Delta E_{\text{CCSD}}^{\text{rcc}}$) and triples correlation energy ($\Delta E_{\text{(T)}}$) are of comparable importance: on the order of a few kcal/mol and systematically favoring the LS and IS state with respect to the HS one. Although relativistic effects and the effect of outer-core correlation were not determined separately in all cases (because this is not needed in our computational protocol), based on a few cases studied, the effect of core correlation appears more important than the relativistic effects. This observation is consistent with estimates of relativistic effects on the relative spin-state energetics at the DFT level (cf Table S2), being often as small as 1 kcal/mol or less.

As compared with the previous coupled cluster studies of heme-related mimics,^{16,19,21} the presently discussed set of spin-state energetics contains a larger number of systems, all treated consistently using the same methodology, with minimal basis set error and the metal outer-core correlation included. Note that Table 2 also give results for two much larger complexes with the porphyrin ring—FeP and FeP(Cl)—to illustrate that the protocol described in section 4.1 can be applied not only to small mimics but also to more realistic models. Further applications will be presented in forthcoming papers.

Three of the present models, FeA₂(SH), FeL₂(SH), and FeA₂(NH₃), have been studied at the CCSD(T) level by Olah and Harvey, who carried out the [T:Q]/D extrapolation.^{19a} As concluded in the previous section, the results of the [T:Q]/D extrapolation are affected by an error of several kcal/mol. It is thus intriguing that some of the previous results, particularly for the FeA₂(NH₃) model, resemble the present ones (from ref 19a: ³IS–⁵HS = 17.3, ¹LS–⁵HS = 30.4 kcal/mol; in this work: 16.6 and 29.7 kcal/mol, respectively). However, the cited calculations were performed without correlating the Fe outer-core orbitals (3s,3p), which (in view of our results) is expected to shift up in energy the IS and LS states with respect to the HS state by a few kcal/mol; this error apparently cancels out with the error of the [T:Q]/D extrapolation. Clearly, such an error cancellation has no physical basis and is not expected to be systematic. For instance, much larger discrepancies with the present calculations are observed in the case of FeA₂(SH) (from ref 19a: ⁴IS–⁶HS = 13.9, ²LS–⁶HS = 29.8 kcal/mol; in this work: 10.6 and 21.7 kcal/mol, respectively).

The FeA₂(Cl) model has also been studied before with coupled cluster methods by Ghosh et al.;¹⁶ in fact, it was probably the first heme-related molecule studied at the CCSD(T) level a long time ago. However, as the mentioned calculations were based on a very small orbital basis set (of DZ quality) and took into account neither relativity nor the Fe 3s,3p correlation, the reported ⁴IS–⁶HS splitting of 17 kcal/mol was much overestimated as compared to the 10.5 kcal/mol obtained in this study. The ²LS–⁶HS splitting was not reported in ref 16.

4.3. Multireference Character. In order to judge the quality of a single-reference description—and thus to identify cases where accuracy of the CCSD(T) methods may possibly degrade—several diagnostics of multireference character have

been proposed in the literature: the \mathcal{J}_1 and \mathcal{D}_1 diagnostics (based on amplitudes of the singles at the CCSD level),⁷¹ the %TAE[(T)] diagnostics (i.e., percentage contribution of the connected triples to the CCSD(T) atomization energy),^{24,72} spin contamination at the UCCSD level ($\langle S^2 - S_z^2 - S_z \rangle$), and the largest amplitude of a double excitation in the CCSD wave function, $|t_{2,\text{max}}|$.²⁴ Rough criteria have been proposed for reliable energetics of single-reference calculations for transition metal compounds, namely: $\mathcal{J}_1 < 0.05$, $\mathcal{D}_1 < 0.15$, and %TAE[(T)] < 10%.²⁴ A summary of diagnostics for the models discussed in the previous section can be found in Table 3, whereas the complete data are given in the Supporting Information (Table S17).

Table 3. Summary of Diagnostics for Multireference Character^a

diagnostics	median value	largest value(s)	worst offender(s)
\mathcal{J}_1	0.027	0.044	FeL ₂ (SH), ¹ LS
		0.044	FeA ₂ (SH), ¹ LS
\mathcal{D}_1	0.127	0.266	FeP(Cl), ¹ LS
		0.265	FeL ₂ (SH), ¹ LS
		0.257	FeA ₂ (SH), ¹ LS
$ t_{2,\text{max}} $		0.068	[FeL ₂ (CN)] [−] , ¹ LS
		0.067	[FeA ₂ (CN)] [−] , ⁵ HS
$\langle S^2 - S_z^2 - S_z \rangle$	0.0048	0.0881	FeA ₂ (Cl), ¹ LS
%TAE[(T)]	2.41	3.42	FeA ₂ (SH), ¹ LS
		3.30	FeA ₂ (Cl), ¹ LS

^aCalculations of the diagnostics with the T/D basis set at the rcc level for all the models included in Table 2. A detailed set of results is available in the Supporting Information (Table S17).

From analysis of this data, it follows that only one of the conditions proposed in ref 24 (i.e., $\mathcal{D}_1 < 0.15$) is violated in a few cases (e.g., the Fe(III) species with Cl or SH axial ligands). However, the %TAE[(T)] and the spin contamination diagnostics always remain pretty small (below 3.5% and 0.02, respectively), and no appreciably large amplitudes of the double excitations do appear. It is noteworthy that relatively large \mathcal{D}_1 values (in spite of small \mathcal{J}_1 and %TAE diagnostics) have been previously found typical of coordination complexes.²⁴ The minute %TAE values seem to indicate that relatively large relaxation of orbitals—i.e., the effect measured by the \mathcal{D}_1 and \mathcal{J}_1 diagnostics—does not necessarily degrade the CCSD(T) energetics.

Moreover, the amplitude diagnostics \mathcal{D}_1 and \mathcal{J}_1 can be much smaller if the calculations are based on the Kohn–Sham (KS) orbitals instead of the HF orbitals, because the KS orbitals are already adapted to electron correlation^{19a,21,73,74} (the results based on the KS orbitals are given in Table S18, Supporting Information). This comes at the price of slightly increased t_2 amplitudes, but $|t_{2,\text{max}}|$ never exceeds 0.1. However, somewhat opposite of the previous results,^{19a} the energetics based on the KS orbitals is not always the same as based on the HF orbitals. For the KS orbitals (as compared with the HF orbitals), the LS and IS states are usually stabilized with respect to the HS state. Although this effect is often very small (0.2–0.5 kcal/mol), much larger discrepancies (up to 2–3 kcal/mol) arise in a few cases, typically marked by elevated $\mathcal{D}_1^{\text{KS}}$ diagnostics (cf. Table S18). Determining which choice of the orbitals (i.e., the HF or the KS ones) gives rise to more accurate energetics is beyond

the scope of this study, but this topic may be worthy of further research.

The ultimate test of the CCSD(T) accuracy would be, clearly, its comparison with higher-order coupled cluster calculations. Unfortunately, the CCSDT calculations (i.e., with full iterative treatment of the triples) are presently too expensive for the models studied, not to mention even more demanding CCSDT(Q) calculations. Nonetheless, CCSD(T) can be compared with the completely renormalized coupled cluster method CR-CC(2,3) of Piecuch et al.⁶⁰ This method provides a different noniterative correction for the connected triples, which can be considered superior to the (T) correction for problematic cases with multireference character, like diradicals and a single bond breaking, where CR-CC(2,3) is able to follow the CCSDT results, even when the accuracy of CCSD(T) is already degraded.⁷⁵ Therefore, sizable discrepancies between the CR-CC(2,3) and CCSD(T) may indicate possible shortcomings of CCSD(T). By contrast, an agreement between both methods may be viewed as a validation of the CCSD(T) energetics.

With this aim in mind, the CCSD(T) and CR-CC(2,3) spin-state energetics are compared for a few A_2 -based models and $FeL_2(SH)$ (Table 4). Before proceeding to the results, it must be noticed that the available implementation of the CR-CC(2,3) method is based on the UCCSD approximation, not on the RCCSD one (mainly used in this work). Since there is

Table 4. Comparison of Relative Spin State Energetics from RCCSD(T), UCCSD(T), and CR-CC(2,3) Methods and \mathcal{D}_1 Diagnostics^a

		RCCSD(T)	UCCSD(T)	CR-CC(2,3)	\mathcal{D}_1
FeA_2	1LS	55.4	56.3	57.1	0.111
	3IS_1	13.2	13.4	13.9	0.119
	3IS_2	18.2	18.5	18.8	0.115
	5HS	0	0	0	0.074
MnA_2	2LS_1	81.0	81.3	81.9	0.093
	2LS_2	57.2	57.4	58.2	0.107
	4IS_1	29.0	27.5	27.4	0.096
	4IS_2	36.5	36.0	36.4	0.104
	6HS	0	0	0	0.061
CoA_2	2LS_1	0	0	0	0.142
	2LS_2	-5.8	-6.1	-5.7	0.147
	4HS_1	-11.1	-11.6	-12.2	0.069
	4HS_2	-8.8	-9.3	-9.9	0.070
$FeA_2(NH_3)$	1LS	34.2	35.0	36.0	0.103
	3IS	18.8	18.7	19.1	0.111
	5HS	0	0	0	0.074
$FeA_2(Cl)$	2LS	33.4	34.7	35.1	0.205
	4IS	11.1	10.6	10.7	0.182
	6HS	0	0	0	0.108
$FeA_2(SH)$	2LS	24.8	26.7	28.3	0.257
	4IS	11.6	11.3	11.4	0.174
	6HS	0	0	0	0.132
$FeL_2(SH)$	2LS	-5.7	-3.9	-1.4	0.265
	4IS	3.0	2.7	2.9	0.163
	6HS	0	0	0	0.150

^aEnergy values in kcal/mol, \mathcal{D}_1 diagnostics from RCCSD. Note that CR-CC(2,3) calculations are based on UCCSD and therefore should be compared with UCCSD(T). The calculations were performed with the T/D basis set at the rcc level.

already a minute difference between the RCCSD(T) and UCCSD(T) energetics, the CR-CC(2,3) energetics is to be compared with the UCCSD(T) one. The second remark: for computation efficiency considerations, the energies in Table 4 were obtained using the T/D basis set, which though too small to provide accurate energetics, is appropriate for comparison of the three similar methods.

From Table 4, it follows that the UCCSD(T) and CR-CC(2,3) relative energetics often agree well, up to 0.5–1 kcal/mol. However, larger discrepancies (up to 2.5 kcal/mol) are observed in a few cases, e.g., for the 1LS state of $FeL_2(SH)$, $FeA_2(SH)$. Interestingly, in these cases there is a noticeable difference already between the RCCSD(T) and UCCSD(T) energetics, as well as elevated \mathcal{D}_1 diagnostics. The diagnostics are, in general, higher for the LS state than for the IS and HS states. Although this trend is understandable, a large variation of the diagnostics should be worrying, as it may indicate that errors due to nondynamical correlation are not comparable for the different spin states, and thus they may poorly cancel out in the relative energetics.

In passing, we note that the deviations of CR-CC(2,3) from UCCSD(T) typically give rise to an opposite effect than that caused by switching from the HF to KS orbitals (which was considered above). Therefore, it would be highly interesting for future studies to determine which approximation (i.e., RCCSD(T), UCCSD(T), or CR-CC(2,3)) and which choice of the orbitals (HF or KS) provide the best agreement with higher-order coupled cluster results. Nonetheless, based on the presented comparison, it is expected that for many cases—such as $FeA_2(NH_3)$ and FeA_2 , and even for the 4IS – 6HS splitting in $FeA_2(SH)$ and $FeL_2(SH)$ —the CCSD(T) energetics should be reliable because the different approximations point to very similar answers (within 1 kcal/mol). On the other hand, there are a few problematic cases—such as the 2LS – 6HS and 2LS – 4IS splittings in $FeA_2(SH)$ and $FeL_2(SH)$ —which may indeed suffer from multireference character (discrepancies between various approximations to CCSDT in Table 4 are larger than 2 kcal/mol). Hence, larger “error bars” have to be put presently on the CCSD(T) results for these few cases.

4.4. Estimates for Heme Models and Comparison with DFT. Although reliable calculations can be performed for simplified, heme-related mimics (see above), it is obvious that these models only loosely resemble the properties of real heme groups. As we shall see, the spin-state energetics of the small mimics are also quite different than for more complete heme models. However, there is typically a remarkable correlation between the spin-state energetics of the full heme model and of its small mimic—when both systems are treated with a number of DFT methods.

This is illustrated in Figure 2 for the two examples: (a) FeP (full heme model)/ FeL_2 (mimic) and (b) FeP(Cl) (full heme model)/ $FeL_2(Cl)$ (mimic). For each pair of models, the results from a number of DFT methods are shown as color points (numeric DFT results can be found in Table S2, Supporting Information). In correlation plots like Figure 2, each color refers to a given spin-state splitting (e.g., 3IS_1 – 5HS); three such relative splittings are considered for FeP/ FeL_2 , only two for FeP(Cl)/ $FeL_2(Cl)$. Analogous correlations can also be observed with the energetics of even simpler mimics, FeA_2 or $FeA_2(Cl)$, as shown in the Supporting Information.

For both pairs of models shown in Figure 2, one can observe that the DFT spin-state energetics are strongly functional-dependent, which is a well-known (and undesired) behav-

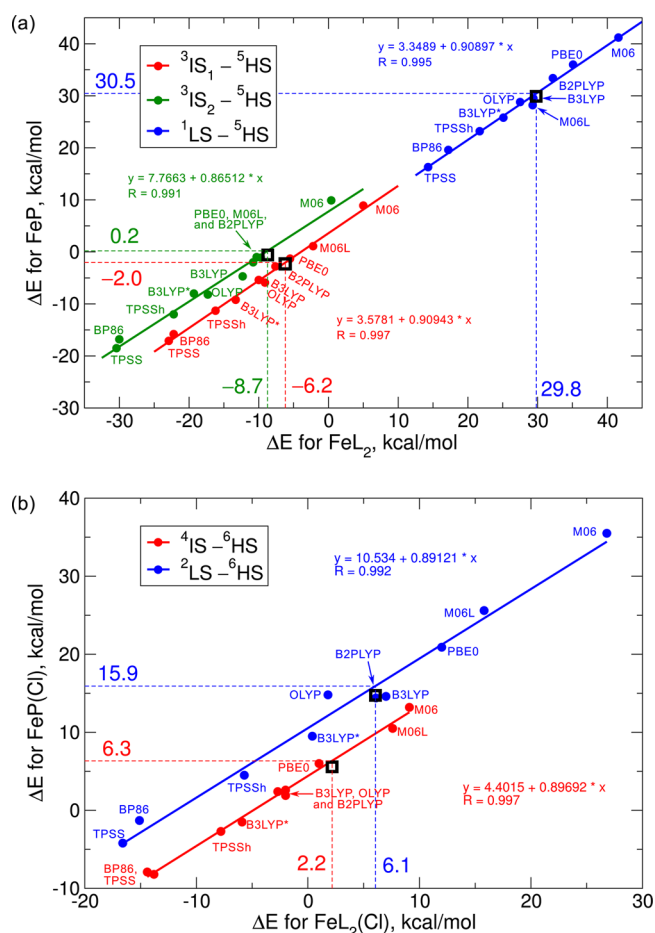


Figure 2. Correlation between spin-state energetics of a full heme model and its small mimic on the example of (a) FeP/FeL₂ and (b) FeP(Cl)/FeL₂(Cl). The DFT relative energies obtained from 10 different functionals for each of the considered relative spin-state energetics are shown as color points (numeric DFT results are available in the Supporting Information). The fitted trend lines (whose equations and correlation coefficients are shown) are used to estimate the energetics for the full heme model based on the CCSD(T) results for the respective small mimic (dashed lines, annotated values). The actual CCSD(T) energetics are shown as black, empty squares.

ior.^{4,11,12} Nonetheless, it can be observed that a functional which underestimates or overestimates the relative energetics for the full heme model behaves in the same way also for the small mimic. Hence, there is a nearly quantitative correspondence between the energetics of both models obtained from different functionals, resulting in a high value of the correlation coefficient. Such a regular behavior (which is also observed for other heme models, see below) justifies the use of simplified mimics for benchmarking of DFT methods with the aim of applying them to the full heme complexes.

The observed correlation can be even more profitable if noticed that most of the DFT points lie close (within the chemical accuracy) to the corresponding trend lines. This suggests use of the trend line for making predictions concerning the full heme model based on the accurate energetics for its small mimic (coming from the present coupled cluster or other *ab initio* calculations). This procedure is illustrated for both examples in Figure 2. Clearly, such a prediction gives merely an estimate of the energetics, and it cannot substitute performing high-level calculations for the large model. But since the latter

are often unfeasible or very expensive, such an estimate can be valuable.

The present approach may be compared to a hybrid method, such as ONIOM with two layers. As in the latter methodology, we combine accurate energetics of the small mimic, calculated at the CCSD(T) level, with a model correction (i.e., difference between the full model and the mimic), estimated at the DFT level. But different from the ONIOM approach, a number of DFT methods are used here to establish the model correction—the correction is reflected in both the slope (*a*) and the intercept (*b*) of the fitted trend line ($y = ax + b$). The present approach would be equivalent to ONIOM if $a = 1$, meaning that a single DFT calculation would be enough to provide the model correction (which would be then the *b* parameter). Although *a* is not far from unity, it is typically somewhat smaller, meaning that the mimic slightly over-emphasizes discrepancies between different DFT methods; this effect is taken into account by the linear fit. We further note the recent work of Lawson Daku et al., who estimated the spin-state energetics of large complexes, [Co(tpy)₃]²⁺ and [Co(bpy)₂]²⁺, based on the accurate CCSD(T) calculations for a smaller complex [Co(NCH)₆]²⁺ (from ref 23) and a series of DFT calculations for all three complexes and the ligands (to establish an appropriate thermodynamic cycle).⁷⁶ This approach is clearly different from the present estimation procedure, but both approaches explore the potential of DFT methods to properly describe the relationship between energetics of models with different ligands.

Since the CCSD(T) calculations have already been performed for FeP and FeP(Cl) (thanks to the high symmetry of these models, see section 4.2), it is possible to compare the presently proposed estimates with the actually computed results (Table 5). It turns out that the agreement is acceptably good,

Table 5. CCSD(T) Spin-State Energetics of FeP and FeP(Cl): Estimates Based on The Small Mimics and Actual Values^a

model	energetics	estimate based on ^b		actual value ^c
		A ₂ -mimic	L ₂ -mimic	
FeP	¹ LS– ⁵ HS	30.3	30.5	29.9
	³ IS ₁ – ⁵ HS	–1.1	–2.0	–2.3
	³ IS ₂ – ⁵ HS	0.6	0.2	–0.6
FeP(Cl)	² LS– ⁶ HS	19.7	15.9	14.7
	⁴ IS– ⁶ HS	7.7	6.3	5.6

^aAll values in kcal/mol. ^bMaking use of the linear correlations in Figure 2 or similar ones with the energetics of FeA₂ or FeA₂(Cl) (which are shown in the Supporting Information). ^cEnergies from Table 2.

particularly for the estimates based on the L₂-mimics (confirming our presumption that these larger mimics are better models of heme groups). This, obviously, does not prove that the CCSD(T) energetics are accurate in the absolute sense, but it is noteworthy that they are consistent with the trend lines established from a series of DFT calculations (see the black squares in Figure 2). At least in these two examples where the actual CCSD(T) energetics have been obtained, the “statistical error” arising from the estimation procedure seems to be acceptable, below 2 kcal/mol when using the L₂-mimics (but larger for the smaller A₂-mimics, as might be expected). This encouraged us to apply this approach also to other heme models, for the sake of comparing with experimental spin-state

data (wherever available) and discussing the DFT performance in the following sections.

4.4.1. Metalloporphyrins, $M = \text{Fe(II)}$, Mn(II) , Co(II) . The results for the models of iron(II) porphyrin (full model FeP, small mimic FeL_2) have already been presented and partly discussed (cf. Table 5, Figure 2a). The CCSD(T) method clearly points to the triplet ground state for FeP, which is consistent with the interpretation of experimental data of four-coordinate iron(II) porphyrins.⁷⁷ The present CCSD(T) energetics of the quintet and triplet states are in good agreement with the recent CASPT2 calculations,²⁶ based on a large active space (including not only selected valence orbitals but also the Fe outer-core orbitals), where the following relative energies were found for FeP (kcal/mol): $^3\text{IS}_1 - ^5\text{HS} = -0.9$ and $^3\text{IS}_2 - ^5\text{HS} = 1.4$. Both studies also agree on the high-lying ^1LS state.

It should be mentioned that the relative energetics of triplet and quintet spin states of FeP used to be a subject of major controversy.²⁶ While nearly all DFT calculations give the correct (triplet) ground state, most of the ab initio calculations (prior to ref 26a) pointed to the wrong (quintet) ground state.^{6a,26b,78} It was even suggested that the experimental data of FeP might have been misinterpreted.^{78a} However, a quality treatment of electron correlation (like in ref 26a and in the present study) gives the ground state of FeP in agreement with the experimental data.

While all tested DFT methods (except M06) correctly point to the triplet ground state, they give highly variable splittings between the spin states. Concerning the $^3\text{IS}_1 - ^5\text{HS}$ and $^3\text{IS}_2 - ^5\text{HS}$ relative energies, the best agreement with CCSD(T) is achieved for PBE0 and B2PLYP functionals. The B3LYP energetics are also satisfactory (slight overstabilization of the triplets by 3–4 kcal/mol), as well as the M06L one (overstabilization of the quintet with respect to $^3\text{IS}_1$ by 3 kcal/mol). However, the B3LYP* and TPSSh functionals (as well as OLYP, concerning the $^3\text{IS}_2 - ^5\text{HS}$ energy difference) give rise to overstabilization of the triplet state with respect to the quintet state by more than 6 kcal/mol. The situation is slightly different for the $^1\text{LS} - ^5\text{HS}$ energy difference, where the best agreement with CCSD(T) (within ~ 2 kcal/mol) is obtained for B3LYP, OLYP, M06L, and B2PLYP functionals.

However, from the experimental point of view, more important than this high-energy singlet state are the low-lying quintet and triplet states. In this regard, it is noteworthy that all nonhybrid functionals (BP86, OLYP, TPSS, M06L) and even TPSSh (10% of exact exchange) place the orbitally degenerate triplet state $^3\text{IS}_2$ (i.e., 3E_g) slightly below the orbitally nondegenerate one, $^3\text{IS}_1$ (i.e., $^3A_{2g}$). Although some experimental data of FeP were interpreted in favor of the 3E_g ground state,^{77c} this is supported neither by the present CCSD(T) nor by the previous CASPT2 calculations. In reality, the two triplet states are so close in energy that they significantly mix with each other if spin–orbit interaction is taken into account.^{26a} This effect makes it impossible to interpret the experimental data of Fe(II) porphyrins in terms of either a pure $^3A_{2g}$ or 3E_g ground state.

The analogous correlation plots for manganese(II) and cobalt(II) porphyrins compared with their small mimics (MnL_2 and MnA_2 and CoL_2 and CoA_2) are given in Figures S3–S6 (Supporting Information). The experimental ground state is, respectively, doublet for CoP and sextet for MnP,⁷⁹ which is correctly recovered by the present CCSD(T) estimates. The doublet ground state of CoP ($^2\text{LS}_1$) is also correctly reproduced

by all the tested functionals, although the actual value of the quartet–doublet relative energy is strongly functional-dependent. B3LYP and B2PLYP give the best agreement with the CCSD(T) results ($^4\text{HS}_{1,2} - ^2\text{LS}_1$ of 12.5 and 12.7 kcal/mol, respectively, calculated for CoL_2 ; 10.8 and 8.7 kcal/mol, respectively, estimated for CoP). By contrast, the experimental sextet (^6HS) spin state of MnP cannot be reproduced by many functionals (including B3LYP*, OLYP, and TPSSh), which instead strongly favor the degenerate quartet ($^4\text{IS}_2$) spin state by more than 10 kcal/mol as compared with CCSD(T). Interestingly, the CCSD(T) estimates place both quartet states ($^4\text{IS}_1$, $^4\text{IS}_2$) at high energy above the sextet ground state ($^4\text{IS}_{1,2} - ^6\text{HS}$ splitting of 10.8 and 6.3 kcal/mol, respectively, calculated for MnL_2 ; 11.1 and 9.8 kcal/mol, respectively, estimated for MnP). It turns out that only few functionals (M06, B2PLYP, and PBE0) can follow the CCSD(T) energetics reasonably well, with discrepancies smaller than 5 kcal/mol.

4.4.2. Pentacoordinate Fe(II) Complexes. Figure 3 shows the spin-state energetics of FeP(Im), a model of the ferrous active site in deoxymyoglobin,^{6a,80,81} vis-à-vis the energetics of its small mimic, $\text{FeL}_2(\text{NH}_3)$. The structures of both models are additionally shown (panel a), as well as schematic occupancies

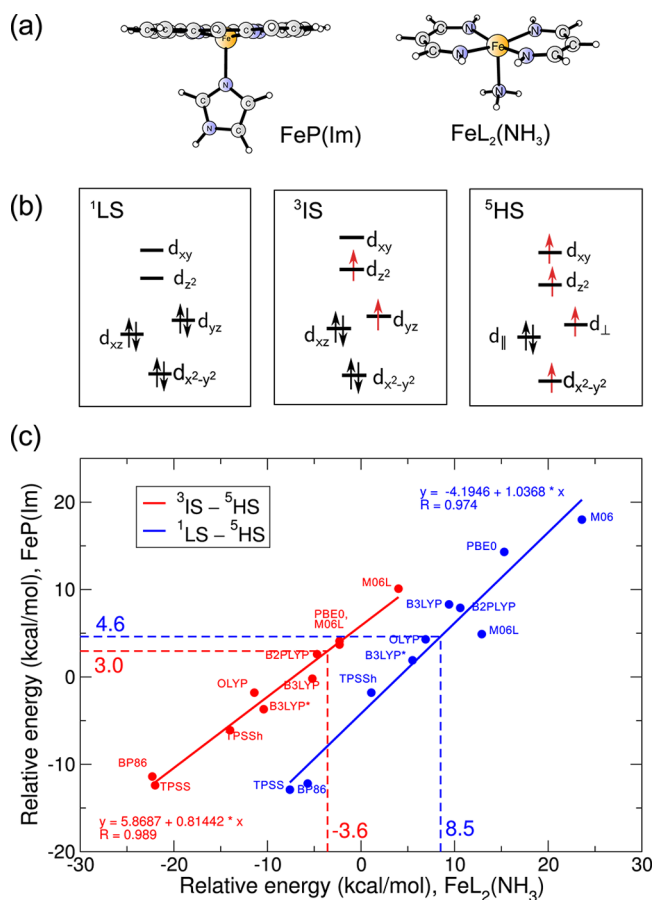


Figure 3. Structures of the FeP(Im) complex and its small mimic $\text{FeL}_2(\text{NH}_3)$ (a); schematic occupancies of the Fe 3d orbitals in the ^1LS , ^3IS , and ^5HS states of both models (b); and correlation between the FeP(Im) and $\text{FeL}_2(\text{NH}_3)$ spin-state energetics obtained from variety of DFT methods (c). Numeric DFT results can be found in the Supporting Information. Annotated are the CCSD(T) energetics for $\text{FeL}_2(\text{NH}_3)$ and the resulting estimates for FeP(Im).

of the orbitals in their ^1LS , ^3IS , and ^5HS states (panel b). Looking at panel c of the figure, one may notice that the ^1LS – ^5HS relative energies of $\text{FeP}(\text{Im})$ and $\text{FeL}_2(\text{NH}_3)$ correlate much worse than in the previous examples. In fact, three of the tested functionals (B3LYP, B2PLYP, M06L) predict the ^1LS – ^5HS relative energy in different order for $\text{FeL}_2(\text{NH}_3)$ than for $\text{FeP}(\text{Im})$. Consequently, the fitted trend line has limited significance and cannot be used for making precise predictions. However, taking into account the results of OLYP, B3LYP, B2PLYP, and M06L—the four functionals which most closely resemble the CCSD(T) value of the ^1LS – ^5HS splitting in $\text{FeL}_2(\text{NH}_3)$ —one can roughly estimate the analogous ^1LS – ^5HS splitting in $\text{FeP}(\text{Im})$ as 4–8 kcal/mol. The estimate based on the smaller mimic $\text{FeA}_2(\text{NH}_3)$ also falls in this range (see Figure S7, Supporting Information). In contrast to the ^1LS – ^5HS splitting, the linear correlation is much better for the ^3IS – ^5HS energy difference, thus allowing to make a more precise estimate of it (~ 3 kcal/mol) for $\text{FeP}(\text{Im})$. Taking into account a slightly higher estimate resulting from comparison with the $\text{FeA}_2(\text{NH}_3)$ mimic (cf Figure S7), the ^3IS – ^5HS splitting for $\text{FeP}(\text{Im})$ can be more safely estimated as 3–5 kcal/mol. This is most correctly reproduced by B2PLYP, M06L, and PBE0, somewhat worse by B3LYP.

The spin-state energetics of $\text{FeP}(\text{Im})$ have already been extensively studied at the CASPT2 level.^{6a,20} It was suggested—based on comparison with the CCSD(T) results for $\text{FeA}_2(\text{NH}_3)$ from Olah and Harvey^{19a}—that the CASPT2 calculations may overstabilize the ^5HS state with respect to the ^1LS and ^3IS states by a few kcal/mol. This is fully confirmed in the present study—based on the improved CCSD(T) methodology and a larger mimic, $\text{FeL}_2(\text{NH}_3)$. The present CCSD(T) estimates (Figure 3c) point to a conclusion that the CASPT2 calculations^{6a,20} could have overestimated the ^1LS – ^5HS splitting by 5–8 kcal/mol and the ^3IS – ^5HS splitting by 3–5 kcal/mol. It is noteworthy that if Kohn–Sham orbitals were used in the present CCSD(T) calculations, as was the case in ref 19a, these discrepancies would be even larger (cf Table S18, Supporting Information). It is unlikely that the present discrepancies between CASPT2 and CCSD(T) energetics indicate a failure of CCSD(T) due to pronounced multi-reference character—the latter is particularly small for $\text{FeA}_2(\text{NH}_3)$ and $\text{FeL}_2(\text{NH}_3)$ models, as was revealed in section 4.3 by inspection of \mathcal{D}_1 and other diagnostics, and by comparison with the CR-CC(2,3) method. It is more likely that these discrepancies are rooted in the weakness of perturbation-theory treatment of dynamical correlation in CASPT2 (at least when this method is used with a standard choice of the active space and the default IPEA shift parameter in the zero-order Hamiltonian).

Unfortunately, the experimental results do not give much information on spin-state energetics for similar, imidazole-ligated Fe(II) porphyrins, except for a clear indication of the quintet ground state,⁸² in line with the present CCSD(T) estimates for $\text{FeP}(\text{Im})$. However, more experimental data are available for a cyanide-ligated Fe(II) porphyrin complex,⁸³ whose model $[\text{FeP}(\text{CN})]^-$ is considered here along with its small mimic, $[\text{FeL}_2(\text{CN})]^-$ (Figure 4). The experimental data of $[\text{Fe}(\text{TPP})(\text{CN})]^-$ (TPP = tetraphenylporphin) reveal a thermal spin crossover from the ^1LS to the ^5HS state, in which the higher-lying ^3IS state does not participate.⁸³ The observation of a spin crossover makes it possible to obtain an

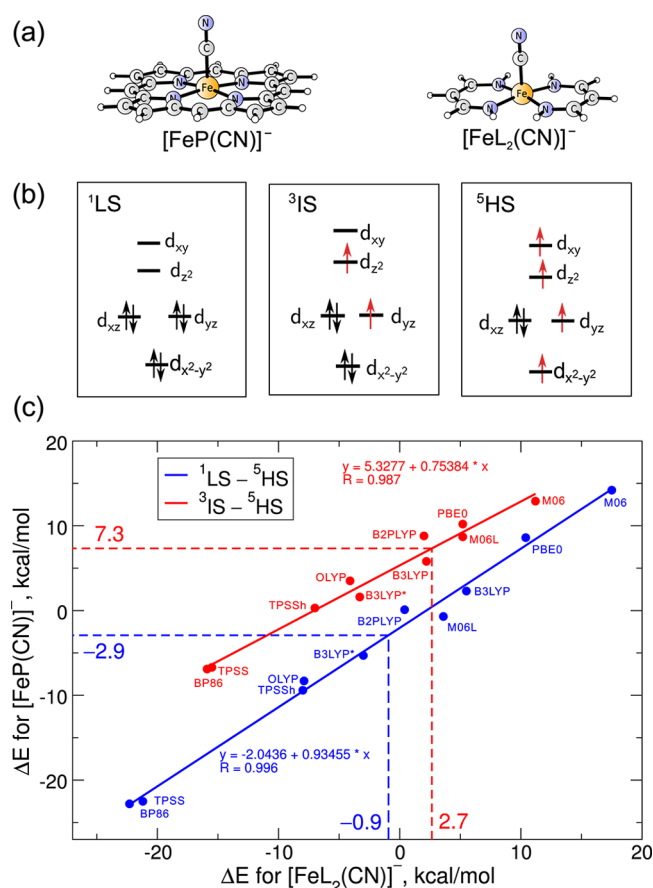


Figure 4. Structures of $[\text{FeP}(\text{CN})]^-$ complex anion and its small mimic $[\text{FeL}_2(\text{CN})]^-$ (a); schematic occupations of the Fe 3d orbitals in the ^1LS , ^3IS , and ^5HS states of both models (b); and correlation between the $[\text{FeP}(\text{CN})]^-$ and $[\text{FeL}_2(\text{CN})]^-$ spin-state energetics from a variety of DFT methods (c). Numeric DFT results can be found in the Supporting Information. Annotated are the results of CCSD(T) calculations for $[\text{FeL}_2(\text{CN})]^-$ and the resulting estimates for $[\text{FeP}(\text{CN})]^-$.

experimental estimate of -5.0 kcal/mol for the electronic energy difference ^1LS – ^5HS .⁸⁴

This experimental ^1LS – ^5HS splitting is best reproduced by the B3LYP* functional (which is not surprising, as this functional was designed to improve spin-state energetics of iron complexes close to the spin-crossover regime⁴⁶). The OLYP and TPSSH functionals also give acceptable results (overstabilization of the ^1LS state by 3–4 kcal/mol), in contrast to B3LYP or PBE0, which underestimates the stability of the ^1LS state by more than 7 kcal/mol. The present CCSD(T) estimate (based on comparison with the $[\text{FeL}_2(\text{CN})]^-$ model, Figure 4c) falls into good agreement with the experimental result. It is presently uncertain whether the discrepancy of ~ 2 kcal/mol (in favor of the HS state) reflects a minor inaccuracy of the CCSD(T) energetics or just a roughness (“statistical error”) of the estimation procedure.⁸⁵ However, we notice that the use of Kohn–Sham orbitals in the CCSD(T) calculations for $[\text{FeL}_2(\text{CN})]^-$ gives rise to extra stabilization of the ^1LS and ^3IS states with respect to the ^5HS state by ~ 3 kcal/mol (cf. Table S18, Supporting Information); considering this effect would improve the agreement with the experimental ^1LS – ^5HS energetics.

All in all, comparison with the experimental data for $\text{FeP}(\text{Im})$ and $[\text{FeP}(\text{CN})]^-$ shows that the change of spin-state due to

different axial ligation in these complexes is properly accounted for by the CCSD(T) method.

4.4.3. Pentacoordinate Fe(III) Complexes. A spin-crossover behavior is also observed for the pentacoordinate ferric state of the P450 active site (after removing a water molecule from the resting state of the enzyme⁹), whose simplified model FeP(SH) is considered here, along with the small mimic FeL₂(SH) (Figure 5). The experimental data for the ferric form P450 are

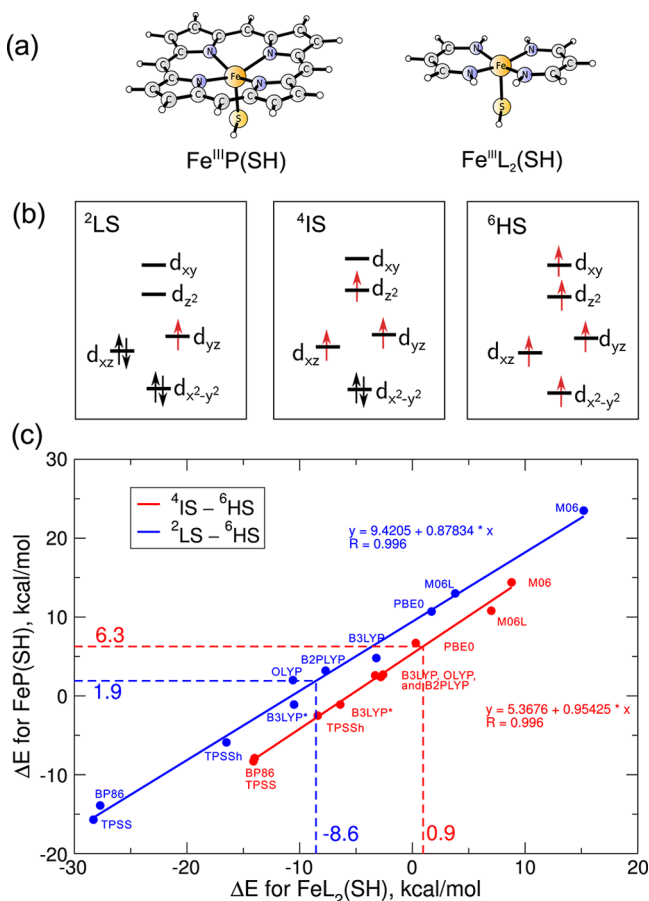


Figure 5. Structures of the FeP(SH) complex and its small mimic FeL₂(SH) (a); schematic occupations of the Fe 3d orbitals in the ²LS, ⁴IS, ⁶HS electronic states of both models (b); and correlation between the FeP(SH) and FeL₂(SH) spin state energetics obtained from variety of DFT methods (c). Numeric DFT results can be found in the Supporting Information. Annotated are the results of CCSD(T) calculations for FeL₂(SH) and the resulting estimates for FeP(SH).

interpreted in terms of thermal equilibrium between the close lying doublet (²LS) and sextet (⁶HS) states, in which the quartet (⁴IS) state does not participate.⁸⁶ Such a state ordering is in agreement with the present CCSD(T) estimates (cf Figure 5c).

Indeed, the ²LS and ⁶HS states of FeP(SH) are predicted very close in energy, well below the ⁴IS state, consonant with the fact that the latter state is not significantly populated at room temperature.⁸⁶ In fact, given that the present CCSD(T) energetics for FeP(SH) are only an estimate (based on the results for the small mimic), the ²LS state may well be located slightly below the ⁶HS state, as suggested by the experimental data in ref 86 (in particular $\Delta H_{LS-HS} < 0$ and the spin-crossover behavior, normally indicative of the LS below the HS state).

It is surprisingly difficult to obtain the experimental state ordering (i.e., ²LS \sim ⁶HS $<$ ⁴IS) from DFT calculations. While various functionals lead to very different relative energetics, they typically either strongly stabilize or destabilize both the ²LS and the ⁴IS states with respect to the ⁶HS state. Intriguingly, the ⁴IS state is often predicted nearly degenerate with ²LS and sometimes even below it, which contradicts the experimental state ordering. Such a behavior was previously observed for B3LYP,⁸⁷ but in view of the present results it is also the case of many other functionals (e.g., B3LYP*, B2PLYP, PBE0, M06L). These problems with a simultaneously correct description of the ²LS–⁶HS and ⁴IS–⁶HS energetics may be rooted in a different degree of covalency for the metal bonding with the axial ligand (Fe–SH) than with the equatorial ligand (Fe–porphyrin).

Clearly, the experimental state ordering was determined for the pentacoordinate ferric form of the P450 enzyme and does not apply directly to the presently studied FeP(SH) model. However, the effect of protein environment on the spin state energetics was investigated by Altun and Thiel⁸⁷ (at the DFT:B3LYP level), and this effect *does not* seem to account for the observed discrepancies. Indeed, the data in ref 87 suggest that the ⁴IS state of the enzymatic site is stabilized with respect to ⁶HS by ~ 1.5 kcal/mol, while the ²LS state is destabilized with respect to the ⁶HS state by ~ 2 kcal/mol, as compared with the present FeP(SH) model in the gas phase. It means that once the protein environment is correctly taken into account, the DFT energetics are even more biased in favor of the low-lying ⁴IS state!

The similar overstabilization of the IS state can also be observed for another pentacoordinate Fe(III) complex, namely FeP(Cl), for which the CCSD(T) and DFT results were already given above (see Figure 2b and Table 5). Although experimental data of its octaethylporphyrin analogue, Fe(OEP)-(Cl), clearly point to the ⁶HS ground state well below the ⁴IS and ²LS excited states, a number of historic DFT calculations for FeP(Cl) incorrectly pointed to the ⁴IS ground state or predicted the ⁶HS and ⁴IS states to be nearly degenerate, as discussed by Ghosh and Taylor with their co-workers.¹⁶ The present CCSD(T) value of the ⁴IS–⁶HS splitting (5.6 kcal/mol) is indeed underestimated by B2PLYP, OLYP, and B3LYP and even more considerably by the TPSSH and B3LYP* functionals (cf. Figure 2b). The DFT and CCSD(T) energetics of FeP(Cl) are thus significantly different, although we recognize that—once the model and the methodology of coupled cluster calculations is considerably improved in the present work—the discrepancies are not as large as originally reported.¹⁶ We further notice that the present issue with ferric complexes FeP(SH) and FeP(Cl) may be analogous to a situation of Mn(II) porphyrin (also a d⁵ complex) discussed in section 4.4.1, where many common functionals were found to overstabilize the ⁴IS state with respect to the ⁶HS ground state.

Going back to FeP(SH), it is noteworthy that the present CCSD(T) estimates fall in good agreement with the previous CASPT2 calculations for the same model²⁰ (i.e., ²LS–⁶HS = 3.6 to 4.1 kcal/mol, ⁴IS–⁶HS = 7.5 to 8.7 kcal/mol, data from ref 20). This is in contrast to the situation previously discussed for FeP(Im) and quite remarkable when taking into account the pronounced multireference character in the ²LS state of the tiolate-ligated complexes (see section 4.3). This close agreement, while not being proof of accuracy, suggests that the high D₁ diagnostics may not necessarily degrade a quality of the CCSD(T) energetics. On the other hand, neither the previous

CASPT2 calculations nor the present CCSD(T) estimates point exactly to the expected ^2LS state; however, the present CCSD(T) estimate places this doublet state at slightly lower energy above the sextet state than in the previous CASPT2 calculations. Thus, while there might be, indeed, a problem with the ^2LS – ^6HS splitting for these ferric complexes, it seems that this issue can be resolved neither by CASPT2 calculations (ref 20) nor by switching to a completely renormalized CR-CC(2,3) method (cf. Table 4, section 4.3), because these two approaches place the ^2LS state at even higher energy than according to CCSD(T).

4.4.4. Ferryl Heme Model. The last example covered in this work is a ferryl heme model, $\text{FeO}(\text{P})\text{Cl}$, studied along with its small mimic, $\text{FeO}(\text{L}_2)\text{Cl}$ (Figure 6). These models are relevant

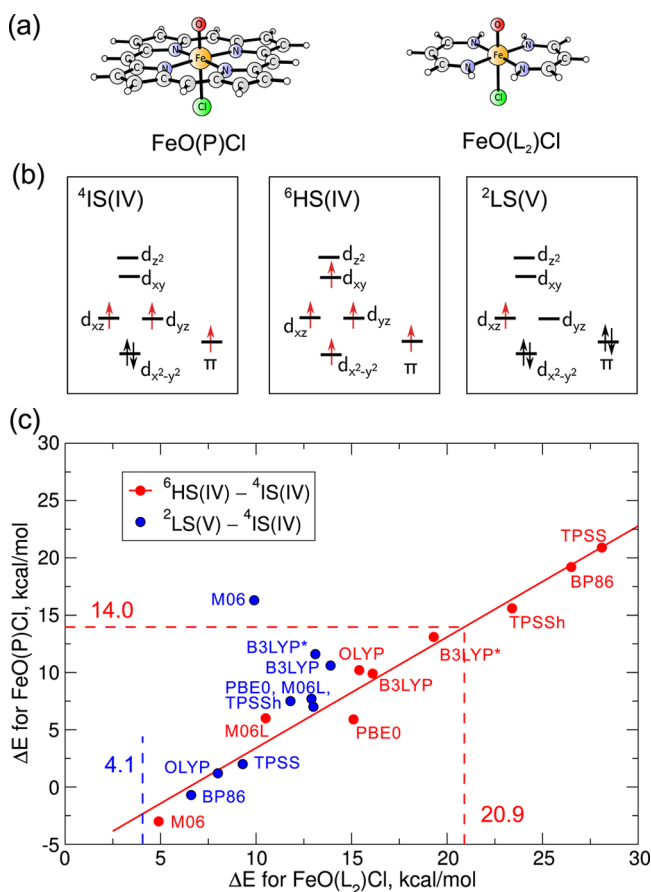


Figure 6. Structures of $\text{FeO}(\text{P})\text{Cl}$ and its small mimic $\text{FeO}(\text{L}_2)\text{Cl}$ (a), schematic occupations of Fe 3d orbitals in their considered electronic states (b), and correlation between their spin state energetics obtained from variety of DFT methods (c). Numeric DFT results can be found in the Supporting Information. Annotated are the results of CCSD(T) calculations for $\text{FeO}(\text{L}_2)\text{Cl}$ and the resulting estimate for $\text{FeO}(\text{P})\text{Cl}$. For the $^2\text{LS(V)} - ^4\text{IS(IV)}$ energetics, no appreciable correlation is observed; hence no estimate is given.

for the electronic structure of high-valent iron-porphyrin species involved in catalytic and enzymatic cycles.^{9,22,88} As compared with P450 Cpd I, they do not contain a soft thiolate ligand (intentionally, to avoid further complications with the description of their electronic structure). In spite of this simplification, it is still possible to identify their electronic states analogous to those of Cpd I,²¹ in particular the Fe(IV) triradicaloid state [$^4\text{IS(IV)}$], the Fe(IV) pentaradicaloid state

[$^6\text{HS(IV)}$], and the Fe(V) state [$^2\text{LS(V)}$] (see Figure 6b and Table S1, Supporting Information).

Although the triradicaloid Fe(IV) ground state is experimentally well established for P450 Cpd I and other high-valent iron porphyrins, the other mentioned states are interesting too, in view of speculations about their role in unusual reactivities of these systems.^{1,22,88,89} Whether this is possible or not depends critically on the relative energetics of these excited states with respect to the ground state. The present calculations of the $^6\text{HS(IV)} - ^4\text{IS(IV)}$ and $^2\text{LS(V)} - ^4\text{IS(IV)}$ energetics for the simplified models are, clearly, not attempting to fully resolve these issues. Their purpose is to shed light on the accuracy of DFT for these important relative energetics in comparison with the CCSD(T) calculations. This is an extension of the previous work for an $[\text{FeO}(\text{L}_2)]^+$ cation²¹—now focused on a more realistic (charge-neutral) model, $\text{FeO}(\text{L}_2)\text{Cl}$, and using the improved CCSD(T) protocol.

Before discussing the results, the reader must be made aware of some technical complications occurring in the CCSD(T) calculations for $\text{FeO}(\text{L}_2)\text{Cl}$. We found that the ROHF calculations for the $^4\text{IS(IV)}$ state can be converged only with great difficulty and to the electronic structure, which does not provide a good starting point for the subsequent CCSD(T) calculations. The problem is that one of the unpaired electrons localizes nearly completely on the oxygen atom; simultaneously a significant spin density is also found on the Cl atom, while the radical character nearly disappears from the cyclic ligand. This happens presumably due to neglect of an electron correlation in the $\text{Fe}=\text{O}$ bond. The problem disappears in the DFT calculations where the correlation is taken into account during the orbital optimization step. Therefore, the present CCSD(T) calculations for $\text{FeO}(\text{L}_2)\text{Cl}$ are based on the Kohn–Sham (KS) orbitals from the RO-B3LYP calculations, instead of the canonical ROHF orbitals. Note that the same choice of orbitals was actually made in ref 21 for $[\text{FeO}(\text{L}_2)]^+$. The use of KS orbitals in CCSD(T) is legitimate,^{19a,74} but the experience gathered for other models in section 4.3 suggests that this approach typically stabilizes the LS and IS states with respect to the HS state by up to 1–3 kcal/mol, as compared with the choice of canonical HF orbitals (cf. Table S18, Supporting Information).

Yet another difference compared with the models studied above is the choice of basis set. Because the L ligands actively participate in the electronic structure of the $^4\text{IS(IV)}$ and $^6\text{HS(IV)}$ states, the calculations were carried out with a basis set of TZ quality on all the ligand atoms instead of a DZ or a mix of DZ and TZ basis set used in the adopted computational protocol. As can be seen from Table S15 (Supporting Information), this extension of the basis set affects the relative energetics of $\text{FeO}(\text{L}_2)\text{Cl}$ by 2–2.5 kcal/mol.

The DFT results for $\text{FeO}(\text{P})\text{Cl}$ and $\text{FeO}(\text{L}_2)\text{Cl}$, along with the CCSD(T) results for the mimic, are shown in Figure 6c. A clear trend can be observed for the $^6\text{HS(IV)} - ^4\text{IS(IV)}$ energetics,⁹⁰ but not for the $^2\text{LS(V)} - ^4\text{IS(IV)}$ one (see below). Concerning the $^6\text{HS(IV)} - ^4\text{IS(IV)}$ energy gap, the CCSD(T) result for the small model can be translated into an estimate of ~ 14 kcal/mol for $\text{FeO}(\text{P})\text{Cl}$. This is somewhat higher than that according to B3LYP (10 kcal/mol), closer to B3LYP* (13 kcal/mol) and TPSSH (16 kcal/mol). However, in this case, the CCSD(T) calculations are based on the KS orbitals—suggesting that the $^6\text{HS(IV)} - ^4\text{IS(IV)}$ energy difference may be overestimated by 1–3 kcal/mol as compared with (hypothetical) calculations based on the canonical HF orbitals

(see above). Therefore, it is still difficult to judge the precise value of the ${}^6\text{HS}(\text{IV})$ – ${}^4\text{IS}(\text{IV})$ gap, although the B3LYP or OLYP results (~ 10 kcal/mol) are to be considered reliable, if not underestimated by a few kcal/mol. In contrast, the results from M06, M06L, and PBE0 functionals—as well as those from the CASPT2 and RASPT2 calculations of ref 21 (i.e., 3.2 and -1.5 kcal/mol, respectively)—suggest that these method considerably overstabilize the pentaradicaloid state with respect to the triradicaloid ground state by more than 8 kcal/mol (this behavior of CASPT2 may be analogous to over stabilization of the HS state for FeP(Im), mentioned in section 4.4.2).

As mentioned above, for the second energy difference in Figure 6c, i.e., ${}^2\text{LS}(\text{V})$ – ${}^4\text{IS}(\text{IV})$, there is no appreciable linear correlation between the DFT results for the full model and the small mimic. This problem illustrates a limitation of our approach, but it was not unexpected. The transition between the ${}^4\text{IS}(\text{IV})$ and ${}^2\text{LS}(\text{V})$ states is not like typical spin promotions considered so far, because it involves an intermolecular charge transfer between the ring and the iron-oxo group (i.e., change of the iron oxidation number).

Although the trend line cannot be fitted for the ${}^2\text{LS}(\text{V})$ – ${}^4\text{IS}(\text{IV})$ relative energy, it is intriguing that the CCSD(T) result for the small mimic is only 4.0 kcal/mol. This is lower than according to any DFT method tested, implying (at first sight) that the ${}^2\text{LS}(\text{V})$ state is placed at very low energy and could be even the ground state of FeO(P)Cl. A few comments must be made at this stage. First, this result is consonant with our previous study,²¹ where the low-lying Fe(V) electromer was found for $[\text{FeO}(\text{P})]^+$ and FeO(P)Cl in the gas phase on the basis of CASPT2 and RASPT2 calculations for these models and $[\text{FeO}(\text{L}_2)]^+$, supported by CCSD(T) calculations for the latter mimic. However, it was also found that gas-phase calculations underestimate by a few kcal/mol the stability of the Fe(IV) states with respect to the Fe(V) states, as compared with the situation in polarizable media.²¹ Thus, the present estimate for FeO(P)Cl does not automatically point to the Fe(V) ground state (which would contradict the experimental data for similar complexes, as discussed in ref 21) but rather to the presence of a low-energy excited state with an Fe(V) character. The similar low-lying Fe(V) states were also reported by Chen et al. in their CASPT2/MM calculations for P450 Cpd I.²²

The second remark concerns the reliability of the CCSD(T) energetics for FeO(L₂)Cl. Whereas the ${}^4\text{IS}(\text{IV})$ and ${}^6\text{HS}(\text{IV})$ states have the D_1 diagnostics of 0.052 and 0.067, respectively, a much higher value of 0.132 is found for the ${}^2\text{LS}(\text{V})$ state. This suggests more significant multireference character in the ${}^2\text{LS}(\text{V})$ state than in the other states, and this is a warning sign indicating a possible deterioration of the CCSD(T) accuracy. However, we notice that multireference calculations (CASPT2, RASPT2)—where these potential problems with static correlation are addressed appropriately—also place the Fe(V) states at low energy.^{21,22} The qualitative agreement between the single- and multireference calculations cannot be ignored: it suggests that the low-energy Fe(V) state may be realistic. However, further ab initio calculations are necessary to fully clarify this issue.

5. CONCLUSIONS AND OUTLOOK

This work was focused on elucidating the spin-state energetics of metalloporphyrin complexes and biologically relevant heme

groups by means of coupled cluster calculations for their simplified mimics.

In order to efficiently calculate the relative spin-state energetics at the CCSD(T) level, a practical computational protocol was proposed—based on the mix of explicitly correlated (F12) methodology and extrapolation to the complete basis set—where basis sets are used economically, particularly for calculation of the most expensive connected triples contribution $[(T)]$ to the correlation energy. The accuracy of this approach was verified by comparison with a more expensive CBS extrapolation for selected small models (the agreement typically better than 1 kcal/mol, maximum discrepancy 1.6 kcal/mol). However, a small cost makes this protocol applicable also to much larger complexes, which was illustrated by performing CCSD(T) calculations for FeP and FeP(Cl) (P = porphyrin); further applications will be presented in forthcoming papers.

It was also shown that CCSD(T) results for simplified mimics can be used to estimate the spin-state energetics of the corresponding larger models—even if the latter may be presently too large for high-level ab initio calculations—once a relation between both models is established at the DFT level. The resulting CCSD(T) estimates turned out to be (within 1–2 kcal/mol) consistent with the actual CCSD(T) results for FeP and FeP(Cl), and in accord with the experimental spin-state data available for the considered porphyrin complexes and heme groups. This approach was also applied to study the excited states of the ferryl heme model, with the stress on the relative energies of the triradicaloid and the pentaradicaloid state, and of the Fe(V) electromer.

Another goal of this work was to compare the CCSD(T) results with predictions of various DFT methods. In some cases the results of commonly used functionals (e.g., B3LYP, B3LYP*, B2PLYP) were supported, but in general none of the tested DFT methods provided a consistently good agreement with CCSD(T) for all the studied models. Intriguingly, this may hold true even for different spin-state energetics within the same system—like for the case of FeP(SH), where it seems very difficult to provide a realistic energetics simultaneously for the three spin states (the doublet, quartet, and sextet) by simply changing the exchange correlation functional. This may imply the need of benchmarking DFT not just for a given system or class of systems but rather for a given class of relative spin-state energetics.

Due to intense development of local correlation methods, coupled cluster calculations are becoming possible for larger and more complicated models than could be imagined just a few years ago.^{31,32b} Moreover, thanks to the F12 approach, convergence with respect to the basis set can be much improved,²⁹ as was also demonstrated in this study. In fact, the present work, likewise ref 23, reveals that already within a traditional (nonlocal) approach to electron correlation it is now possible to perform reliable CCSD(T) calculations (basis set error below 1–2 kcal/mol) for relatively large transition metal systems. In this spirit, it was interesting to see benchmark results and estimates for heme models relevant in (bio)-inorganic chemistry. However, of equal importance is to recognize potential deficiencies in the CCSD(T) energetics due to multireference character in some of the studied systems. The present work, including the analysis of multireference character and comparison with completely renormalized CR-CC(2,3) calculations, suggests that the problems with multireference character are not very severe and their energetics consequences

may not exceed an error bar of ~ 2 kcal/mol usually assumed for CCSD(T) relative energetics. Nonetheless, comparison with higher-order coupled cluster calculations will be interesting, particularly for a few potentially problematic cases, such as tiolate-ligated ferric complexes, identified in the course of this study.

■ ASSOCIATED CONTENT

● Supporting Information

Details of the electronic states, numeric DFT results, additional CCSD(T) results, the remaining correlation plots, and complete ref 58. This material is available free of charge via the Internet at <http://pubs.acs.org/>.

■ AUTHOR INFORMATION

Corresponding Author

*E-mail: mraddon@chemia.uj.edu.pl.

Notes

The authors declare no competing financial interest.

■ ACKNOWLEDGMENTS

This work was supported by grant no. IP2011 044471 from Ministry of Science and Higher Education, Poland; by the POWIEW project (HPC Infrastructure for Grand Challenges of Science and Engineering Project, co-financed by the ERDF under the Innovative Economy Operational Program); and by Foundation for Polish Science under the START program. Supercomputing time from ACK CYFRONET (Zeus cluster), the PL-GRID infrastructure, and WCSS (grant number 181) is gratefully acknowledged. The author is thankful to Prof. Ewa Broclawik and Prof. Tomasz Borowski (J. Haber Institute of Catalysis PAS) for critical reading of the manuscript and valuable suggestions.

■ REFERENCES

- (1) Shaik, S.; Chen, H.; Janardanan, D. *Nat. Chem.* **2011**, *3*, 19–27.
- (2) Deeth, R. J.; Anastasi, A. E.; Wilcockson, M. J. *J. Am. Chem. Soc.* **2010**, *132*, 6876–6877.
- (3) (a) Carréo-Macedo, J.-L.; Harvey, J. N. *J. Am. Chem. Soc.* **2004**, *126*, 5789–5797. (b) Harvey, J. N. *J. Am. Chem. Soc.* **2000**, *122*, 12401–12402.
- (4) (a) Swart, M. *Int. J. Quantum Chem.* **2013**, *113*, 2–7. (b) Costas, M.; Harvey, J. N. *Nat. Chem.* **2013**, *5*, 7–9.
- (5) Franzen, S. *Proc. Natl. Acad. Sci. U. S. A.* **2002**, *99*, 16754–16759.
- (6) (a) Radoń, M.; Pierloot, K. *J. Phys. Chem. A* **2008**, *112*, 11824–11832. (b) Radoń, M.; Broclawik, E.; Pierloot, K. *J. Phys. Chem. B* **2010**, *114*, 1518–1528.
- (7) Borowski, T.; Noack, H.; Radoń, M.; Zych, K.; Siegbahn, P. E. M. *J. Am. Chem. Soc.* **2010**, *132*, 12887–12898.
- (8) Siegbahn, P.; Borowski, T. *Acc. Chem. Res.* **2006**, *39*, 729–738.
- (9) (a) Shaik, S.; Cohen, S.; Wang, Y.; Chen, H.; Kumar, D.; Thiel, W. *Chem. Rev.* **2010**, *110*, 949–1017. (b) Shaik, S.; Kumar, D.; de Visser, S. P.; Altun, A.; Thiel, W. *Chem. Rev.* **2005**, *105*, 2279–2328.
- (10) Cramer, C. J.; Truhlar, D. G. *Phys. Chem. Chem. Phys.* **2009**, *11*, 10757–10816.
- (11) (a) Harvey, J. N. *Annu. Rep. Prog. Chem., Sect. C: Phys. Chem.* **2006**, *102*, 203–226. (b) Harvey, J. N. *Struct. Bonding (Berlin)* **2004**, *112*, 151–183.
- (12) (a) Ghosh, A. *J. Biol. Inorg. Chem.* **2006**, *11*, 712–724. (b) Ghosh, A.; Taylor, P. R. *Curr. Opin. Chem. Biol.* **2003**, *2003*, 113–124.
- (13) Radoń, M.; Broclawik, E. In *Computational Methods to Study the Structure and Dynamics of Biomolecules and Biomolecular Processes - from Bioinformatics to Molecular Quantum Mechanics*; Liwo, A., Ed.; Springer: Berlin, 2014; pp 711–782.

- (14) Chen, H.; Lai, W.; Shaik, S. *J. Phys. Chem. B* **2011**, *115*, 1727–1742.
- (15) Harvey, J. N. *J. Biol. Inorg. Chem.* **2011**, *16*, 831–839.
- (16) (a) Ghosh, A.; Persson, B. J.; Taylor, P. R. *J. Biol. Inorg. Chem.* **2003**, *8*, 507–511. (b) Ghosh, A.; Vangberg, T.; Gonzalez, E.; Taylor, P. J. *J. Porphyrins Phthalocyanines* **2001**, *5*, 345–356.
- (17) (a) Pierloot, K.; Vancoillie, S. *J. Chem. Phys.* **2006**, *125*, 124303. (b) Pierloot, K.; Vancoillie, S. *J. Chem. Phys.* **2008**, *128*, 034104.
- (18) (a) Pápai, M.; Vankø, G.; de Graaf, C.; Rozgonyi, T. *J. Chem. Theory Comput.* **2013**, *9*, 509–519. (b) Kepenekian, M.; Robert, V.; Le Guennic, B. *J. Chem. Phys.* **2009**, *131*, 114702. (c) Kepenekian, M.; Robert, V.; Le Guennic, B.; De Graaf, C. *J. Comp. Chem.* **2009**, *30*, 2327–2333.
- (19) (a) Olah, J.; Harvey, J. *J. Phys. Chem. A* **2009**, *113*, 7338–7345. (b) Strickland, N.; Harvey, J. N. *J. Phys. Chem. B* **2007**, *111*, 841–852.
- (20) Vancoillie, S.; Zhao, H.; Radoń, M.; Pierloot, K. *J. Chem. Theory Comput.* **2010**, *6*, 576–582.
- (21) Radoń, M.; Broclawik, E.; Pierloot, K. *J. Chem. Theory Comput.* **2011**, *7*, 898–908.
- (22) Chen, H.; Song, J.; Lai, W.; Wu, W.; Shaik, S. *J. Chem. Theory Comput.* **2010**, *6*, 940–953.
- (23) Lawson Daku, L. M.; Aquilante, F.; Robinson, T. W.; Hauser, A. *J. Chem. Theory Comput.* **2012**, *8*, 4216–4231.
- (24) Jiang, W.; DeYonker, N. J.; Wilson, A. K. *J. Chem. Theory Comput.* **2011**, *8*, 460–468.
- (25) (a) Andersson, K.; Malmqvist, P.-Å.; Roos, B. O. *J. Chem. Phys.* **1991**, *96*, 1218–1226. (b) Malmqvist, P.-Å.; Pierloot, K.; Shahi, A. R. M.; Cramer, C. J.; Gagliardi, L. *J. Chem. Phys.* **2008**, *128*, 204109.
- (26) (a) Vancoillie, S.; Zhao, H.; Tran, V. T.; Hendrickx, M. F. A.; Pierloot, K. *J. Chem. Theory Comput.* **2011**, *7*, 3961–3977. (b) Pierloot, K. *Mol. Phys.* **2003**, *101*, 2083–2094.
- (27) Bartlett, R. J.; Musial, M. *Rev. Mod. Phys.* **2007**, *79*, 291–352.
- (28) Hughes, T. F.; Harvey, J. N.; Friesner, R. A. *Phys. Chem. Chem. Phys.* **2012**, *14*, 7724–7738.
- (29) Bross, D. H.; Hill, J. G.; Werner, H.-J.; Peterson, K. A. *J. Chem. Phys.* **2013**, *139*, 094302.
- (30) Jiang, W.; DeYonker, N. J.; Determan, J. J.; Wilson, A. K. *J. Phys. Chem. A* **2012**, *116*, 870–885.
- (31) Riplinger, C.; Neese, F. *J. Chem. Phys.* **2013**, *138*, 034106.
- (32) (a) Li, W.; Piecuch, P. *J. Phys. Chem. A* **2010**, *114*, 8644–8657. (b) Kozłowski, P. M.; Kumar, M.; Piecuch, P.; Li, W.; Bauman, N. P.; Hansen, J. A.; Lodowski, P.; Jaworska, M. *J. Chem. Theory Comput.* **2012**, *8*, 1870–1894.
- (33) Johansson, M. P.; Sundholm, D. *J. Chem. Phys.* **2004**, *120*, 3229–3236.
- (34) Scherlis, D. A.; Estrin, D. A. *Int. J. Quantum Chem.* **2002**, *87*, 158–166.
- (35) (a) Hättig, C.; Klopper, W.; Köhn, A.; Tew, D. P. *Chem. Rev.* **2012**, *112*, 4–74. (b) Kong, L.; Bischoff, F. A.; Valeev, E. F. *Chem. Rev.* **2012**, *112*, 75–107.
- (36) Rovira, C.; Kunc, K.; Hutter, J.; Ballone, P.; Parrinello, M. *J. Phys. Chem. A* **1997**, *101*, 8914–8925.
- (37) TURBOMOLE, V6.1–6.3; University of Karlsruhe and Forschungszentrum Karlsruhe GmbH: Karlsruhe, Germany, 1989–2007; TURBOMOLE GmbH: Karlsruhe, Germany, since 2007. Available from <http://www.turbomole.com> (accessed Feb 2014).
- (38) Frisch, M. J.; Trucks, G. W.; Schlegel, H. B.; Scuseria, G. E.; Robb, M. A.; Cheeseman, J. R.; Scalmani, G.; Barone, V.; Mennucci, B.; Petersson, G. A.; Nakatsuji, H.; Caricato, M.; Li, X.; Hratchian, H. P.; Izmaylov, A. F.; Bloino, J.; Zheng, G.; Sonnenberg, J. L.; Hada, M.; Ehara, M.; Toyota, K.; Fukuda, R.; Hasegawa, J.; Ishida, M.; Nakajima, T.; Honda, Y.; Kitao, O.; Nakai, H.; Vreven, T.; Montgomery, J. A., Jr.; Peralta, J. E.; Ogliaro, F.; Bearpark, M.; Heyd, J. J.; Brothers, E.; Kudin, K. N.; Staroverov, V. N.; Kobayashi, R.; Normand, J.; Raghavachari, K.; Rendell, A.; Burant, J. C.; Iyengar, S. S.; Tomasi, J.; Cossi, M.; Rega, N.; Millam, J. M.; Klene, M.; Knox, J. E.; Cross, J. B.; Bakken, V.; Adamo, C.; Jaramillo, J.; Gomperts, R.; Stratmann, R. E.; Yazyev, O.; Austin, A. J.; Cammi, R.; Pomelli, C.; Ochterski, J. W.; Martin, R. L.; Morokuma, K.; Zakrzewski, V. G.; Voth, G. A.; Salvador, P.;

- Dannenberg, J. J.; Dapprich, S.; Daniels, A. D.; Farkas, O.; Foresman, J. B.; Ortiz, J. V.; Cioslowski, J.; Fox, D. J. *Gaussian 09*, revision C.01.; Gaussian, Inc.: Wallingford, CT, 2009.
- (39) Weigend, F.; Ahlrichs, R. *Phys. Chem. Chem. Phys.* **2005**, *7*, 3297–3305.
- (40) Conradie, J.; Ghosh, A. *J. Phys. Chem. B* **2007**, *111*, 12621–12624.
- (41) Güell, M.; Luis, J. M.; Solà, M.; Swart, M. J. *Phys. Chem. A* **2008**, *112*, 6384–6391.
- (42) Weigend, F.; Furche, F.; Ahlrichs, R. *J. Chem. Phys.* **2003**, *119*, 12753–12762.
- (43) Weigend, F.; Häser, M.; Patzelt, H.; Ahlrichs, R. *Chem. Phys. Lett.* **1998**, *294*, 143–152.
- (44) (a) Becke, A. D. *J. Chem. Phys.* **1993**, *98*, 5648–5652. (b) Stephens, P. J.; Devlin, F. J.; Chabalowski, C. F.; Frisch, M. J. *J. Phys. Chem.* **1994**, *98*, 11623–11627.
- (45) Perdew, J. P.; Ernzerhof, M.; Burke, K. *J. Chem. Phys.* **1996**, *105*, 9982–9985.
- (46) Reiher, M.; Salomon, O.; Hess, B. A. *Theor. Chem. Acc.* **2001**, *107*, 48–55.
- (47) Perdew, J. P.; Tao, J.; Staroverov, V. N.; Scuseria, G. E. *J. Chem. Phys.* **2004**, *120*, 6898–6911.
- (48) (a) Becke, A. D. *Phys. Rev. A* **1988**, *38*, 3098–3100. (b) Perdew, J. P. *Phys. Rev. B* **1986**, *33*, 8822–8824.
- (49) Tao, J.; Perdew, J. P.; Staroverov, V. N.; Scuseria, G. E. *Phys. Rev. Lett.* **2003**, *91*, 146401–146404.
- (50) Handy, N. C.; Cohen, A. J. *Mol. Phys.* **2001**, *99*, 403–412.
- (51) Grimme, S. *J. Chem. Phys.* **2006**, *124*, 034108.
- (52) (a) Zhao, Y.; Truhlar, D. G. *J. Phys. Chem. A* **2006**, *110*, 13126–13130. (b) Zhao, Y.; Truhlar, D. G. *J. Chem. Phys.* **2006**, *125*, 194101.
- (53) Siegbahn, P. E. M. *J. Biol. Inorg. Chem.* **2006**, *11*, 695–701.
- (54) (a) Swart, M.; Groenhof, A. R.; Ehlers, A. W.; Lammerstma, K. *J. Phys. Chem. A* **2004**, *108*, 5479–5483. (b) Swart, M. J. *Chem. Theory Comput.* **2008**, *4*, 2057–2066.
- (55) Jensen, K. P. *Inorg. Chem.* **2008**, *47*, 10357–10365.
- (56) Ye, S.; Neese, F. *Inorg. Chem.* **2010**, *49*, 772–774.
- (57) Reiher, M.; Wolf, A. *J. Chem. Phys.* **2004**, *121*, 10945–10956.
- (58) Werner, H.-J. et al. *MOLPRO*, version 2010.1; version 2012.1; Cardiff University: Cardiff, U. K.; Universität Stuttgart: Stuttgart, Germany, 2010. See <http://www.molpro.net> (accessed Feb 2014).
- (59) (a) Knowles, P. J.; Hampel, C.; Werner, H.-J. *J. Chem. Phys.* **1993**, *99*, 5219–5227. (b) Knowles, P. J.; Hampel, C.; Werner, H.-J. *J. Chem. Phys.* **2000**, *112*, 3106–3107.
- (60) (a) Piecuch, P.; Wloch, M. *J. Chem. Phys.* **2005**, *123*, 224105. (b) Wloch, M.; Gour, J. R.; Piecuch, P. *J. Phys. Chem. A* **2007**, *111*, 11359–11382. (c) Shen, J.; Piecuch, P. *Chem. Phys.* **2012**, *401*, 180–202.
- (61) Schmidt, M. W.; Baldridge, K. K.; Boatz, J. A.; Elbert, S. T.; Gordon, M. S.; Jensen, J. H.; Koseki, S.; Matsunaga, N.; Nguyen, K. A.; Su, S.; Windus, T. L.; Dupuis, M.; Montgomery, J. A. *J. Comput. Chem.* **1993**, *14*, 1347–1363.
- (62) (a) Dunning, T. H. *J. Chem. Phys.* **1989**, *90*, 1007–1023. (b) Balabanov, N. B.; Peterson, K. A. *J. Chem. Phys.* **2005**, *123*, 064107.
- (63) Helgaker, T.; Klopper, W.; Koch, H.; Noga, J. *J. Chem. Phys.* **1997**, *106*, 9639–9646.
- (64) (a) Adler, T. B.; Knizia, G.; Werner, H.-J. *J. Chem. Phys.* **2007**, *127*, 221106. (b) Knizia, G.; Adler, T. B.; Werner, H.-J. *J. Chem. Phys.* **2009**, *130*, 054104.
- (65) Werner, H.-J.; Adler, T. B.; Manby, F. R. *J. Chem. Phys.* **2007**, *126*, 164102.
- (66) Marchetti, O.; Werner, H.-J. *Phys. Chem. Chem. Phys.* **2008**, *10*, 3400–3409.
- (67) Weigend, F. *J. Comput. Chem.* **2008**, *29*, 167–175.
- (68) (a) Weigend, F.; Köhn, A.; Hättig, C. *J. Chem. Phys.* **2002**, *116*, 3175–3183. (b) Hill, J. G.; Platts, J. A. *J. Chem. Phys.* **2008**, *128*, 044104.
- (69) The recommendations in this matter by Prof. Kirk A. Peterson and Dr. Gerald Knizia, posted to the Molpro user mailing list, are gratefully acknowledged.
- (70) Although thorough efficiency benchmarks were not performed in this study, it seems that the CCSD-F12 calculations are more than 2 times faster than the corresponding CBS extrapolations that provide a comparable accuracy (Table S14, Supporting Information).
- (71) (a) Lee, T. J.; Taylor, P. R. *Int. J. Quantum Chem.* **1989**, *36*, 199–207. (b) Janssen, C. L.; Nielsen, I. M. B. *Chem. Phys. Lett.* **1998**, *290*, 423–430. (c) Lee, T. J. *Chem. Phys. Lett.* **2003**, *372*, 362–367.
- (72) (a) Karton, A.; Rabinovich, E.; Martin, J. M. L.; Ruscic, B. *J. Chem. Phys.* **2006**, *125*, 144108. (b) Karton, A.; Daon, S.; Martin, J. M. *Chem. Phys. Lett.* **2011**, *510*, 165–178.
- (73) Harvey, J. N.; Aschi, M. *Faraday Discuss.* **2003**, *124*, 129–143.
- (74) Beran, G. J. O.; Gwaltney, S. R.; Head-Gordon, M. *Phys. Chem. Chem. Phys.* **2003**, *5*, 2488–2493.
- (75) Piecuch, P.; Wloch, M.; Gour, J. R.; Kinal, A. *Chem. Phys. Lett.* **2006**, *418*, 467–474.
- (76) Vargas, A.; Krivokapic, I.; Hauser, A.; Lawson Daku, L. M. *Phys. Chem. Chem. Phys.* **2013**, *15*, 3752–3763.
- (77) (a) Collman, J. P.; Hoard, J. L.; Kim, N.; Lang, G.; Reed, C. A. *J. Am. Chem. Soc.* **1975**, *97*, 2676–2681. (b) Goff, H.; La Mar, G. N.; Reed, C. A. *J. Am. Chem. Soc.* **1977**, *99*, 3641–3646. (c) Obara, S.; Kashiwagi, H. *J. Chem. Phys.* **1982**, *77*, 3155.
- (78) (a) Choe, Y.-K.; Nakajima, T.; Hirao, K.; Lindh, R. *J. Chem. Phys.* **1999**, *111*, 3837–3845. (b) Choe, Y.-K.; Hashimoto, T.; Nakano, H.; Hirao, K. *Chem. Phys. Lett.* **1998**, *295*, 380–388.
- (79) (a) Madura, P.; Scheidt, W. R. *Inorg. Chem.* **1976**, *15*, 3182–3184. (b) Kirner, J. F.; Reed, C. A.; Scheidt, W. R. *J. Am. Chem. Soc.* **1977**, *99*, 1093–1101.
- (80) Blomberg, L. M.; Blomberg, M. R.; Siegbahn, P. E. *J. Inorg. Biochem.* **2005**, *99*, 949–958.
- (81) Liao, M.-S.; Huang, M.-J.; Watts, J. D. *J. Phys. Chem. A* **2010**, *114*, 9554–9569.
- (82) (a) Hu, C.; Roth, A.; Ellison, M.; An, J.; Ellis, C.; Schulz, C.; Scheidt, W. *J. Am. Chem. Soc.* **2005**, *127*, 5675–5688. (b) Hu, C.; An, J.; Noll, B. C.; Schulz, C. E.; Scheidt, W. R. *Inorg. Chem.* **2006**, *45*, 4177–4185.
- (83) (a) Li, J.; Lord, R.; Noll, B.; Baik, M.-H.; Schulz, C.; Scheidt, W. *Angew. Chem., Int. Ed.* **2008**, *47*, 10144–10146. (b) Li, J.; Peng, Q.; Barabanschikov, A.; Pavlik, J. W.; Alp, E. E.; Sturhahn, W.; Zhao, J.; Sage, J. T.; Scheidt, W. R. *Inorg. Chem.* **2012**, *51*, 11769–11778.
- (84) As described elsewhere,^{6b} the difference of electronic energy between the spin states is equal to the negative of a thermodynamical free energy correction to the relative energy of both states (including also zero-point vibrational energy), the correction being calculated for the spin crossover temperature, here $T_{1/2} = 265$ K from ref 83a.
- (85) We notice that the estimate based on the smaller mimic $[\text{FeA}_2(\text{CN})]^-$ (Figure S8, Supporting Information) is in worse agreement with the experimental data, as it predicts the ^1LS state slightly above the ^5HS state. However, the experience gained previously for $\text{FeP}(\text{Cl})$ suggests that the estimates based on the L_2 -mimic should be superior to the estimate based on the A_2 -mimic. What are the precise CCSD(T) energetics of $[\text{FeP}(\text{CN})]^-$ remain uncertain until calculations at this level can be afforded for the full heme model.
- (86) Sligar, S. G. *Biochemistry* **1976**, *15*, 5399–5406.
- (87) Altun, A.; Thiel, W. *J. Phys. Chem. B* **2005**, *109*, 1268–1280.
- (88) Pan, Z.; Wang, Q.; Sheng, X.; Horner, J. H.; Newcomb, M. *J. Am. Chem. Soc.* **2009**, *131*, 2621–2628.
- (89) Isobe, H.; Yamaguchi, K.; Okumura, M.; Shimada, J. *J. Phys. Chem. B* **2012**, *116*, 4713–4730.
- (90) For the $^6\text{HS}(\text{IV})$ – $^4\text{IS}(\text{IV})$ energetics, only the B2PLYP results stand out from other functionals, which is due to large spin contamination occurring in the B2PLYP calculations for the $^6\text{HS}(\text{IV})$ state of $\text{FeO}(\text{P})\text{Cl}$, making the results unreliable. For this reason, the B2PLYP energetics are not used to determine the DFT trend line, but they can be found in Table S2, Supporting Information.

■ NOTE ADDED AFTER ASAP PUBLICATION

The Acknowledgments were updated on May 30, 2014.